Table 2. (Continued).

Treatment	Feature Num†	Probe ID‡	Accession Num	Gene	Description	Fold Change
PBO-Treatment						
	38281	89	NM_012575	Grin2c	Glutamate [NMDA] receptor subunit epsilon-3 precursor	5455
	22477	89	NM_012575	Grin2c	Glutamate [NMDA] receptor subunit epsilon-3 precursor	4397
	10081	89	NM_012575	Grin2c	Glutamate [NMDA] receptor subunit epsilon-3 precursor	3207
	18912	89	NM_012575	Grin2c	Glutamate [NMDA] receptor subunit epsilon-3 precursor	2504
	25095	89	NM_012575	Grin2c	Glutamate [NMDA] receptor subunit epsilon-3 precursor	1918
	17400	89	NM_012575	Grin2c	Glutamate [NMDA] receptor subunit epsilon-3 precursor	1896
	7800	89	NM_012575	Grin2c	Glutamate [NMDA] receptor subunit epsilon-3 precursor	1822
	18585	89	NM_012575	Grin2c	Glutamate [NMDA] receptor subunit epsilon-3 precursor	1676
	6078	89	NM_012575	Grin2c	Glutamate [NMDA] receptor subunit epsilon-3 precursor	1355
	56	89	NM_012575	Grin2c	Glutamate [NMDA] receptor subunit epsilon-3 precursor	1273
	21517	19684	NM_001025131	Sult2a2_ predicted	Sulfotransferase family 2A, dehydroepiandrosterone (DHEA)-preferring, member 2 (predicted)	447
	26216	6876	NM_012540	Cyp1a1	Cytochrome P450, family 1, subfamily a, polypeptide 1	122
	35061	32139	NM_053840	Ggt1	Gamma-glutamyltransferase 1	117
	40593	6876	NM_012540	Cyp1a1	Cytochrome P450, family 1, subfamily a, polypeptide 1	105
	42653	6876	NM_012540	Cyp1a1	Cytochrome P450, family 1, subfamily a, polypeptide 1	91
	7512	6876	NM_012540	Cyp1a1	Cytochrome P450, family 1, subfamily a, polypeptide 1	73
	23463	6876	NM_012540	Cyp1a1	Cytochrome P450, family 1, subfamily a, polypeptide 1	70

†Feature Num represents Feature Number. Feature Number and ‡Probe ID were obtained from the data sheet for Whole Rat 4x44K oligo DNA microarrays (Agilent Technologies). "Fold Change" represents the level in relation to that of the corresponding gene in the livers of rats fed the basal diet for 13 weeks.

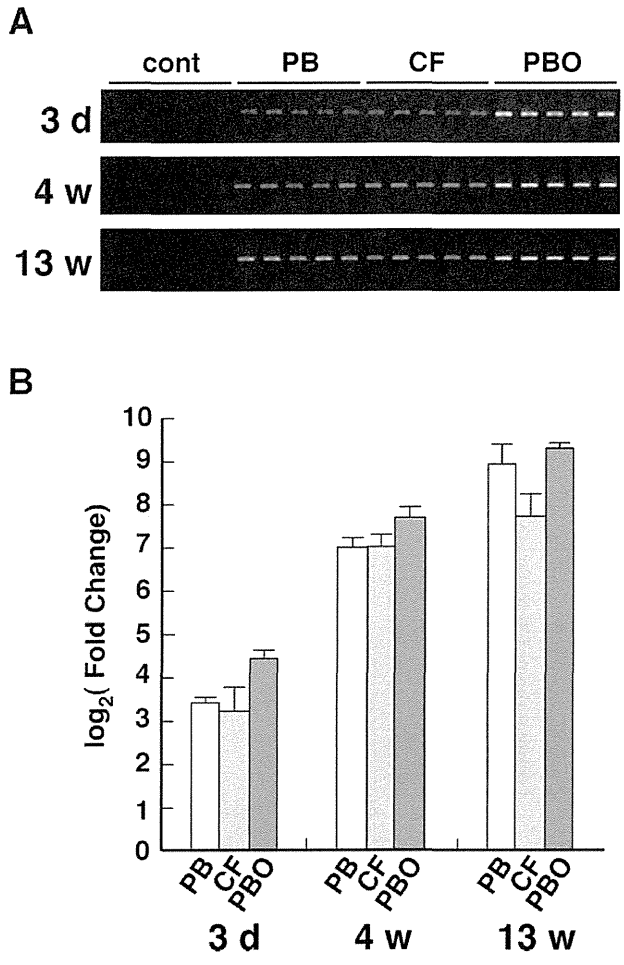

Fig. 2. Expression of the *Grin2c* gene in the livers of rats treated with PB, CF, or PBO. (A) The RT-PCR products from hepatic total RNAs were electrophoresed on a 2 % agarose gel. The lane "cont" represents the product from the RNA in the age-matched rats (control rats). (B) The RNAs used in Panel A were used for real-time RT-PCR analysis. "Fold Change" represents a ratio to the level of the aged-matched control rats. The *Grin2c* mRNA levels were normalized to that of *Gapdh* mRNA. Values are expressed as the means ± S.D. All treatment groups showed significant differences ($p < 0.001$) from the corresponding age-matched control group.

sure of the hepatocarcinogens and liver tumor promoters. To confirm this hypothesis, we intend to further investigate the relationship between the expression of *Grin2c* gene and the proliferation of hepatocytes.

ACKNOWLEDGMENTS

This work was supported in part by a Grant-in-Aid for the Research Program for Risk Assessment Study on Food Safety from the Food Safety Commission, Japan (No. 0703 for K. N., S. O., M. Y., A. N., and M. D.) and a Grant-in-Aid for Scientific Research (C-23590150 for K. N.) from Japan Society for the Promotion of Science.

REFERENCES

Bullock, W.M., Cardon, K., Bustillo, J., Roberts, R.C. and Perrone-Bizzozero, N.I. (2008): Altered expression of genes involved in GABAergic transmission and neuromodulation of granule cell activity in the cerebellum of schizophrenia patients. Am. J. Psychiatry, **165**, 1594-1603.

Cook, J.C. and Hodgson, E. (1985): The induction of cytochrome P-450 by isosafrole and related methylenedioxyphenyl compounds. Chem. Biol. Interact., **54**, 299-315.

Crampton, R.F., Gray, T.J., Grasso, P. and Parke, D.V. (1977): Long-term studies on chemically induced liver enlargement in the rat. I. Sustained induction of microsomal enzymes with absence of liver damage on feeding phenobarbitone or butylated hydroxytoluene. Toxicology, **7**, 289-306.

Elrick, M.M., Kramer, J.A., Alden, C.L., Blomme, E.A., Bunch, R.T., Cabonce, M.A., Curtiss, S.W., Kier, L.D., Kolaja, K.L., Rodi, C.P. and Morris, D.L. (2005): Differential display in rat livers treated for 13 weeks with phenobarbital implicates a role for metabolic and oxidative stress in nongenotoxic carcinogenicity. Toxicol. Pathol., **33**, 118-126.

Fujitani, T., Ando, H., Fujitani, K., Ikeda, T., Kojima, A., Kubo, Y., Ogata, A., Oishi, S., Takahashi, H., Takahashi, O. and Yoneyama, M. (1992): Sub-acute toxicity of piperonyl butoxide in F344 rats. Toxicology, **72**, 291-298.

Hagiwara, A., Miyata, E., Tamano, S., Sano, M., Masuda, C., Funae, Y., Ito, N., Fukushima, S. and Shirai, T. (1999): Non-carcinogenicity, but dose-related increase in preneoplastic hepatocellular lesions, in a two-year feeding study of phenobarbital sodium in male F344 rats. Food Chem. Toxicol., **37**, 869-879.

Hess, R., Stäubli, W. and Riess, W. (1965): Nature of the hepatomegalic effect produced by ethyl-chlorophenoxy-isobutyrate in the rat. Nature, **208**, 856-858.

Hinoi, E., Takarada, T., Ueshima, T., Tsuchihashi, Y. and Yoneda, Y. (2004): Glutamate signaling in peripheral tissues. Eur. J. Biochem., **271**, 1-13.

Huang, W., Zhang, J., Washington, M., Liu, J., Parant, J.M., Lozano, G. and Moore, D.D. (2005): Xenobiotic stress induces hepatomegaly and liver tumors via the nuclear receptor constitutive androstane receptor. Mol. Endocrinol., **19**, 1646-1653.

Kalia, L.V., Kalia, S.K. and Salter, M.W. (2008): NMDA receptors in clinical neurology: excitatory times ahead. Lancet Neurol., **7**, 742-755.

Katsuta, Y., Iida, T., Hasegawa, K., Inomata, S. and Denda, M. (2009): Function of oleic acid on epidermal barrier and calcium influx into keratinocytes is associated with *N*-methyl D-aspartate-type glutamate receptors. Br. J. Dermatol., **160**, 69-74.

Leung, J.C., Marphis, T., Craver, R.D. and Silverstein, D.M. (2004): Altered NMDA receptor expression in renal toxicity: Protection with a receptor antagonist. Kidney Int., **66**, 167-176.

Muguruma, M., Unami, A., Kanki, M., Kuroiwa, Y., Nishimura, J., Dewa, Y., Umemura, T., Oishi, Y. and Mitsumori, K. (2007): Possible involvement of oxidative stress in piperonyl butoxide induced hepatocarcinogenesis in rats. Toxicology, **236**, 61-75.

Nagy, J. (2008): Alcohol related changes in regulation of NMDA receptor functions. Curr. Neuropharmacol., **6**, 39-54.

Parisi, E., Almadén, Y., Ibarz, M., Panizo, S., Cardús, A., Rodriguez, M., Fernandez, E. and Valdivielso, J.M. (2009): *N*-methyl-D-aspartate receptors are expressed in rat parathyroid gland and regulate PTH secretion. Am. J. Physiol. Renal. Physiol., **296**, F1291-1296.

Patsouris, D., Mandard, S., Voshol, P.J., Escher, P., Tan, N.S., Havekes, L.M., Koenig, W., März, W., Tafuri, S., Wahli, W., Müller, M. and Kersten, S. (2004): PPARα governs glycerol metabolism. J. Clin. Invest., **114**, 94-103.

Peters, J.M., Cattley, R.C. and Gonzalez, F.J. (1997): Role of PPARα in the mechanism of action of the nongenotoxic carcinogen and peroxisome proliferator Wy-14,643. Carcinogenesis, **18**, 2029-2033.

Pitot, H.C. (1977): The natural history of neoplasia. Newer insights into an old problem. Am. J. Pathol., **89**, 402-411.

Rao, M.S. and Reddy, J.K. (1991): An overview of peroxisome proliferator-induced hepatocarcinogenesis. Environ. Health Perspect., **93**, 205-209.

Ryu, D.Y., Levi, P.E. and Hodgson, E. (1997): Regulation of hepatic CYP1A isozymes by piperonyl butoxide and acenaphthylene in the mouse. Chem. Biol. Interact., **105**, 53-63.

Rzeski, W., Turski, L. and Ikonomidou, C. (2001): Glutamate antagonists limit tumor growth. Proc. Natl. Acad. Sci. USA, **98**, 6372-6377.

Shimizu, Y., Nakatsuru, Y., Ichinose, M., Takahashi, Y., Kume, H., Mimura, J., Fujii-Kuriyama, Y. and Ishikawa, T. (2000): Benzo[*a*]pyrene carcinogenicity is lost in mice lacking the aryl hydrocarbon receptor. Proc. Natl. Acad. Sci. USA, **97**, 779-782.

Stepulak, A., Luksch, H., Gebhardt, C., Uckermann, O., Marzahn, J., Sifringer, M., Rzeski, W., Staufner, C., Brocke, K.S., Turski, L. and Ikonomidou C. (2009): Expression of glutamate receptor subunits in human cancers. Histochem. Cell Biol., **132**, 435-445.

Takahashi, O., Oishi, S., Fujitani, T., Tanaka, T. and Yoneyama, M. (1994): Chronic toxicity studies of piperonyl butoxide in F344 rats: induction of hepatocellular carcinoma. Fundam. Appl. Toxicol., **22**, 293-303.

Watanabe, K., Kanno, T., Oshima, T., Miwa, H., Tashiro, C. and Nishizaki, T. (2008): The NMDA receptor NR2A subunit regulates proliferation of MKN45 human gastric cancer cells. Biochem. Biophys. Res. Commun., **367**, 487-490.

Waxman, D.J. (1999): P450 gene induction by structurally diverse xenochemicals: central role of nuclear receptors CAR, PXR, and PPAR. Arch. Biochem. Biophys., **369**, 11-23.

Yamamoto, Y., Moore, R., Goldsworthy, T.L., Negishi, M. and Maronpot, R.R. (2004): The orphan nuclear receptor constitutive active/androstane receptor is essential for liver tumor promotion by phenobarbital in mice. Cancer Res., **64**, 7197-7200.

SCIENTIFIC REPORTS

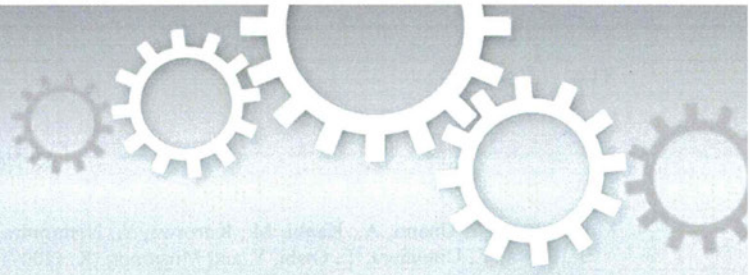

OPEN

SUBJECT AREAS:
MATERIALS
NANOBIOTECHNOLOGY
NANOPARTICLES
BIOMATERIALS

Received
12 March 2012

Accepted
30 April 2012

Published
14 May 2012

Correspondence and requests for materials should be addressed to M.S.X. (msxu@zju.edu.cn) or N.H. (HANAGATA.Nobutaka@nims.go.jp)

Formation of Nano-Bio-Complex as Nanomaterials Dispersed in a Biological Solution for Understanding Nanobiological Interactions

Mingsheng Xu[1], Jie Li[2], Hideo Iwai[3], Qingsong Mei[4], Daisuke Fujita[5], Huanxing Su[6], Hongzheng Chen[1] & Nobutaka Hanagata[2]

[1]State Key Laboratory of Silicon Materials, MOE Key Laboratory of Macromolecule Synthesis and Functionalization & Department of Polymer Science and Engineering, Zhejiang University, Hangzhou 310027, P. R. China, [2]Nanotechnology Innovation Station, National Institute for Materials Science, 1-2-1 Sengen, Tsukuba, Ibaraki 305-0047, Japan, [3]Research Network and Facility Services Division, Materials Analysis Station, National Institute for Materials Science, 1-2-1 Sengen, Tsukuba, Ibaraki 305-0047, Japan, [4]Department of Materials Engineering, School of Powder and Mechanical Engineering, Wuhan University, Wuhan 430072, China, [5]Advanced Key Technologies Research Division, Nano Characterization Unit, National Institute for Materials Science, 1-2-1 Sengen, Tsukuba, Ibaraki 305-0047, Japan, [6]State Key Laboratory of Quality Research in Chinese Medicine and Institute of Chinese Medical Sciences, University of Macau, Macao SAR, China.

Information on how cells interface with nanomaterials in biological environments has important implications for the practice of nanomedicine and safety consideration of nanomaterials. However, our current understanding of nanobiological interactions is still very limited. Here, we report the direct observation of nanomaterial bio-complex formation (other than protein corona) from nanomaterials dispersed in biologically relevant solutions. We observed highly selective binding of the components of cell culture medium and phosphate buffered saline to ZnO and CuO nanoparticles, independent of protein molecules. Our discoveries may provide new insights into the understanding of how cells interact with nanomaterials.

Nanotechnology has held great promise for revolutionizing biomedicine. Nanomaterials (NMs) are widely being under investigation for bioimaging[1], killing tumors[2], delivering drugs/genes[3,4]. The response of biological systems to NMs depends primarily on the surface properties of NMs in a biological environment[5,6]. For example, there is increasing evidence of rapid formation of protein coronas, as NMs within biological environments acquire a coating of protein molecules[7–11], and thus there is some consensus that cellular responses to materials in a biological medium reflect the adsorbed biomolecule layer, rather than the material itself. The concept of the nanoparticle (NP) protein corona is important towards understanding the dynamic surface properties of NMs in biological environments. Unfortunately, the interface issues between NMs and biological systems are too complicated and it is still not very clear how the spontaneous formation of a protein corona influences the materials' interactions with biological systems and contributes to biological outcomes of materials. On the other hand, the increasing use of NMs in industrial and consumer products has aroused global concern regarding their potential impact on the environment and human health. Although a number of studies on the effects of NMs in *in vitro* and *in vivo* systems have been published[12–17], there are still many challenges and issues[12–14] encountered at the interface between NMs and biological systems when assessing the toxicity of NMs. As demonstrated here the state of NMs in biological environments is more complicated than previously thought, requiring a more holistic understanding of what happen as NMs are dispersed in the local biological environments and what cells interface in such an environment. Not only does the biological interface of NMs need to be understood and controlled, but also NMs should be treated as biological entities rather than inorganic ones[6]. The understanding of nano-bio interactions could help in promoting applications of NMs in the biomedical fields and reducing/preventing possible adverse effects to the biological systems caused by NMs.

Here, we present the first report in nanobiological field, to our knowledge, describing nanomaterial (NM) bio-complexes or ion corona formed from the binding of NMs with non-protein components in a biological

environment. We observed highly selective binding of the components of cell culture medium and phosphate buffered saline (PBS) to ZnO and CuO nanoparticles (NPs), independent of protein molecules. Our findings would be helpful to understand nano-bio-interactions, allowing to effectively modifying NM surfaces for specifically biomedical applications.

Results

We observed that ZnO and CuO NPs can bind various constituents from biological environments to form NM bio-complexes or ion corona. The reason that we call the formed clusters as bio-complex is that the NMs are used for biological applications, though it may not involve biological molecules. Figure 1 presents the transmission electron microscopy (TEM) elemental maps of ZnO NPs dispersed in high-glucose Dulbecco's modified Eagle's medium (DMEM) without fetal bovine serum (FBS). In addition to aggregation/agglomeration of the NPs[15], the elemental maps clearly illustrate the binding of ZnO NPs to components of the medium to form NP bio-complexes. We detected Ca, Na, K, P, and Cl originating from the medium (components of DMEM are listed in Supplementary Information). For comparison, we examined the effects of FBS and PBS on the formation of NP bio-complexes. High-resolution TEM images (Fig. 2a and Supplementary Fig. S1) show that in medium supplemented with 10% FBS the crystalline ZnO NPs (see Supplementary Fig. S1) are surrounded by compounds, indicating NP bio-complex formation. Furthermore, we found that these bio-complexes also formed when the ZnO NPs were dispersed in PBS, either with (Supplementary Figs. S2–3) or without FBS (Fig. 2b). We confirmed that the observed highly ordered crystalline structures are ZnO NPs because no crystalline structures were detected in the control suspensions where no ZnO NP was dispersed in medium or PBS (Supplementary Figs. S4–7, S10). These results clearly suggest that the formation of NP bio-complexes in biological environments (medium and PBS) occurs independently of serum proteins. The formation of protein coronas and the adsorption of different proteins onto NPs affect the uptake and transport of NPs in biological systems[7–11]. We believe that the biological behavior of NPs could be similarly modified by the formation of NP bio-complexes.

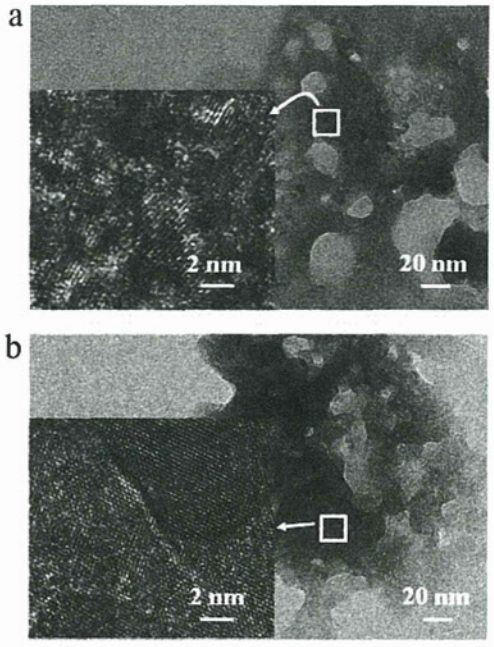

Figure 2 | Surrounded nanoparticles. (a) TEM image of ZnO NPs dispersed in medium supplemented with fetal bovine serum; (b) TEM image of ZnO NPs dispersed in PBS without fetal bovine serum. The inset high-resolution TEM images clearly suggest that ZnO NP (dark-colored) bio-complexes were formed.

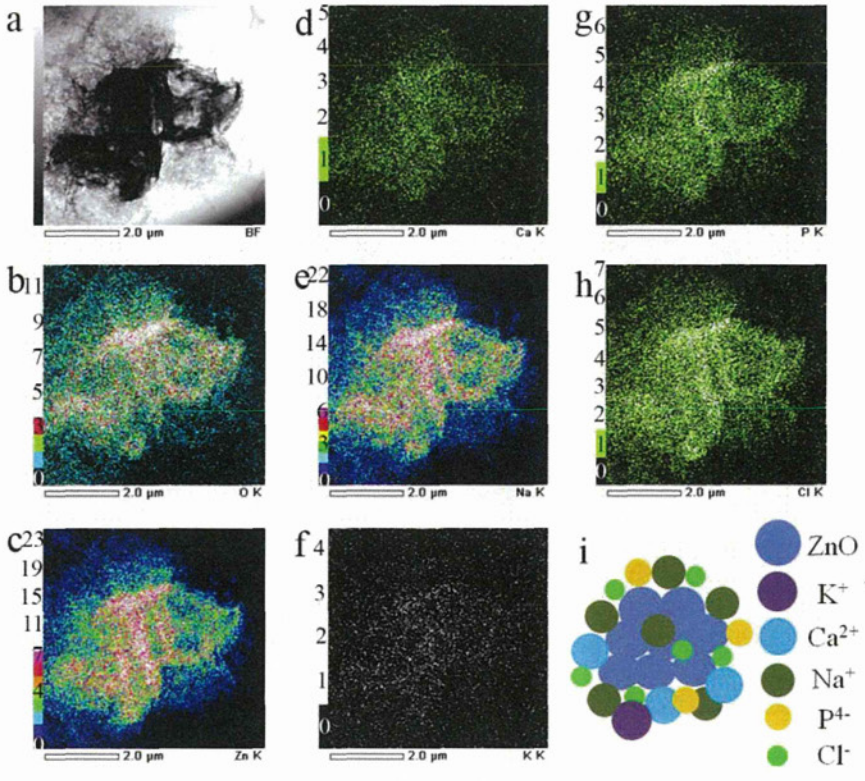

Figure 1 | Formation of ZnO nanoparticle bio-complexes in medium without fetal bovine serum. (a) TEM image showing where the elemental maps were obtained; (b) TEM/EDS O-K map; (c) TEM/EDS Zn-K map; (d) TEM/EDS Ca-K map; (e) TEM/EDS Na-K map; (f) TEM/EDS K-K map; (g) TEM/EDS P-K map; (h) TEM/EDS Cl-K map; (i) A simple model of ZnO bio-complexes.

Figure 3 displays the TEM elemental maps of CuO NPs dispersed in the DMEM supplemented with 10% FBS. By comparing the relative contrast of the maps in Fig. 1 and Supplementary Fig. S1 to that in Fig. 3, we determined that the ZnO and CuO NPs exhibited different binding affinities for the various components of the medium. As plotted in Fig. 4a, in the case of the NPs dispersed in DMEM with FBS, the ZnO NPs bound more Na than Ca and more P than Cl, whereas the CuO NPs bound more Ca than Na and more P than Cl. This selective adsorption may be similar to that seen in the formation of protein coronas, which is reported to be influenced by particle chemistry[9]. Furthermore, FBS has effort on the binding behavior of ions as we can see from Fig. 4a that the ZnO NPs which were dispersed in DMEM with FBS bound more Cl than P, indicating biological environment may also influence the binding process. In addition, as highlighted in Fig. 4b, we observed NP-like clusters that apparently do not contain CuO or ZnO NPs; we believe they arose from components of the cell culture medium. Hence, the bio-complexes and the NP-like clusters can influence size distribution of particles in the biological systems, suggesting caution should be taken as addressing size effects of NMs on biological behaviors.

To confirm the selective binding of ions by the NPs, we used X-ray photoelectron spectroscopy (XPS) to investigate the ensemble of ZnO NPs and CuO NPs after dispersed in the DMEM or DMEM with FBS. Table 1 summarizes the atomic concentrations of the main elements bound by the NPs. In the case of the NPs ensemble dispersed in the DMEM with FBS, the orders of estimated atomic concentration of elements bound by ZnO NPs and by CuO NPs are Na1s (2.8%) > P2s (0.8%) > Ca2p (0.7%) > Cl2p (0.6%) and Na1s (2.6%) > Ca2p (1.8%) > P2s (1.0%) > Cl2p (0.5%), respectively. From Table 1, we also found that FBS affected the ion binding as compared the ZnO NPs dispersed in DMEM to that dispersed in DMEM with FBS. These XPS results are in good agreement with the TEM observation on the individual NPs.

Although we did not detect obvious signal of N, a main component of protein, by TEM, we detected it by XPS due to much lower energy of the used X-ray than the electron beam used for TEM observation. The N1s atomic concentration of the ZnO NPs dispersed in DMEM with FBS is much higher than that of the ZnO NPs dispersed in

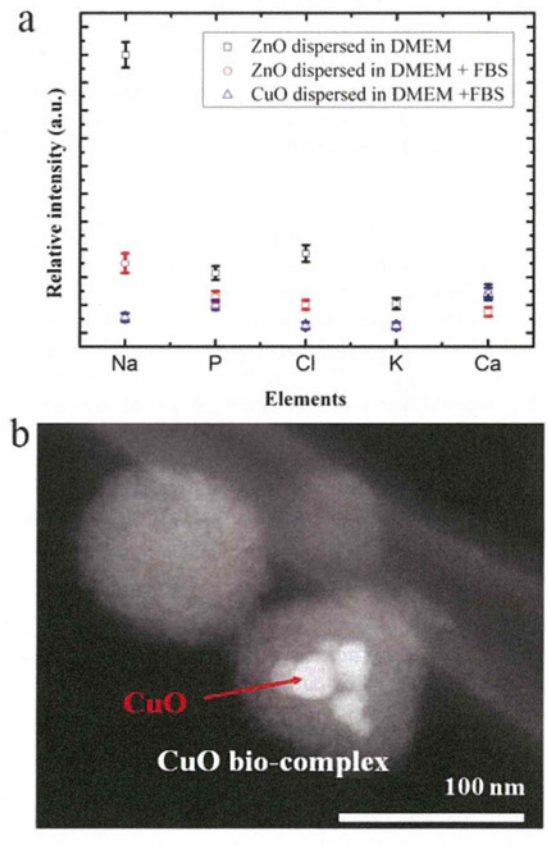

Figure 4 | Selective binding of ions by ZnO and CuO NPs. (a) Scattering plot of bound elements by ZnO and CuO NPs from the DMEM or DMEM with FBS, comparatively showing different binding affinities for the various components of the DMEM or DMEM with FBS by the NPs. The standard deviation error bars were based on the results obtained at three different sample regions; (b) Dark-field TEM image of CuO NPs suspension (25 μg/mL) in medium with FBS, showing nanoparticle-like clusters that apparently do not contain CuO NPs.

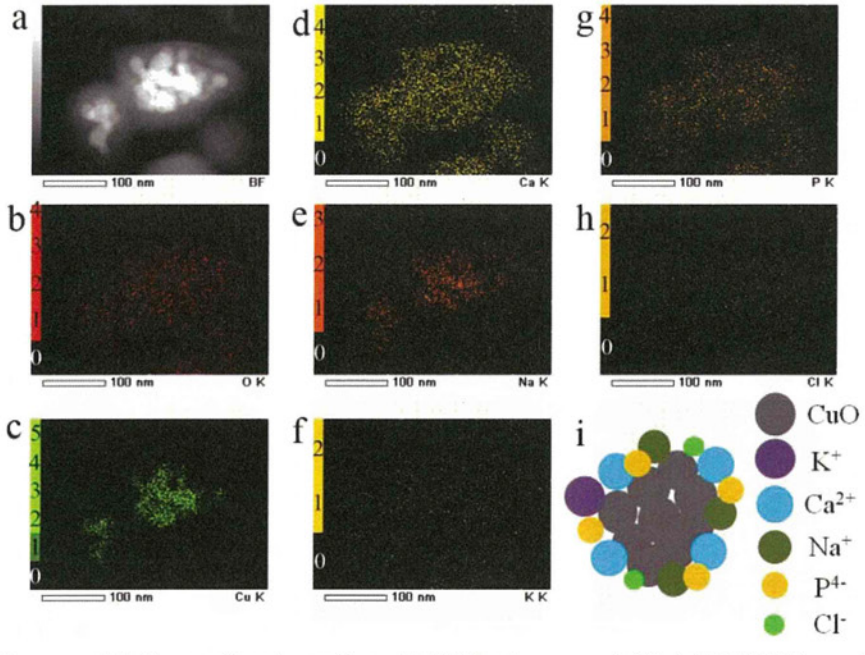

Figure 3 | Formation of CuO nanoparticle bio-complexes in medium with fetal bovine serum. (a) Dark-field TEM image showing where the elemental maps were obtained; (b) TEM/EDS O-K map; (c) TEM/EDS Zn-K map; (d) TEM/EDS Ca-K map; (e) TEM/EDS Na-K map; (f) TEM/EDS K-K map; (g) TEM/EDS P-K map; (h) TEM/EDS Cl-K map; (i) A simple model of CuO bio-complexes.

Table 1 | Atomic concentration (at%) of main elements estimated on the basis of the wide XPS spectra of ZnO and CuO NPs dispersed in DMEM or DMEM with FBS

	N1s	O1s	Na1s	P2s	Cl2p	K2p	Ca2p	Zn2p3/2	Cu2p3/2
#1	2.4	45.6	9.4	1.7	0.7	0.2	2.2	19.5	
#2	9.8	28.0	2.8	0.8	0.5	0.1	0.7	5.4	
#3	10.3	30.1	2.6	1.0	0.5	0.1	1.8		5.9

#1, #2 and #3 represent ZnO NPs dispersed in DMEM, ZnO NPs dispersed in DMEM with FBS and CuO NPs dispersed in DMEM with FBS, respectively.

DMEM. Furthermore, the binding energy of one of the fit peaks of N1s spectra shifted to 399.76 eV (Fig. 5b) or 399.70 eV (Fig. 5c) from 399.41 eV of the pristine FBS (Supplementary Fig. S15b and Table S1). The shift suggests protein molecules in the FBS may bind to the NPs, forming protein corona.

As shown in Figs. 5d–f and Supplementary Figs. S15c–d, we detected different shifts, toward a lower binding energy in contrast to a higher binding energy of the N1s (Figs. 5b–c), of the Na1s and Cl2p binding energies as they contacted with ZnO NPs in DMEM or DMEM with FBS from the pristine DMEM and FBS. The different shift may indicate various interactions between the ions and ZnO NPs in the different solution environments. The various interactions reflect the change of zeta potential of the NPs dispersed in the different solvents as shown in Fig. 6. For instance, the zeta potential of ZnO NPs changed from a negative value in de-ionized water (DI water) to a positive value as dispersed in DMEM or DMEM with FBS. The change of zeta potential of ZnO and CuO NPs is believed to be due to the binding of ions from the solvents, which is consistent with the selective binding of ions by the ZnO and CuO NPs.

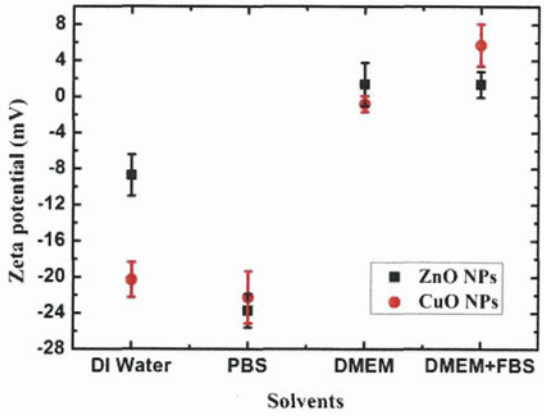

Figure 6 | Various zeta potentials of ZnO and CuO NPs dispersed in different solvents. The change of zeta potential suggests ZnO and CuO NPs bound various ions in the solutions. The error bars represent standard deviation based on three independent measurements of each sample.

Discussion

We have shown that ZnO and CuO NPs formed bio-complex or ion corona by selectively absorbing components or ions from the DMEM, DMEM supplemented with FBS, and PBS. The formation of bio-complexes is not associated with serum proteins. The discovery of bio-complex formation offers new insights for interpreting the observation that the uptake of negatively charged NPs by cells is greater than that of non-functionalized NPs[18,19]. This phenomenon is contradictory to the well-established concept that positively charged NPs have high affinity to the negatively charged cell membrane, and the unfavorable interaction was partially attributed to the formation of NP protein corona[19]. For instance, it has recently been

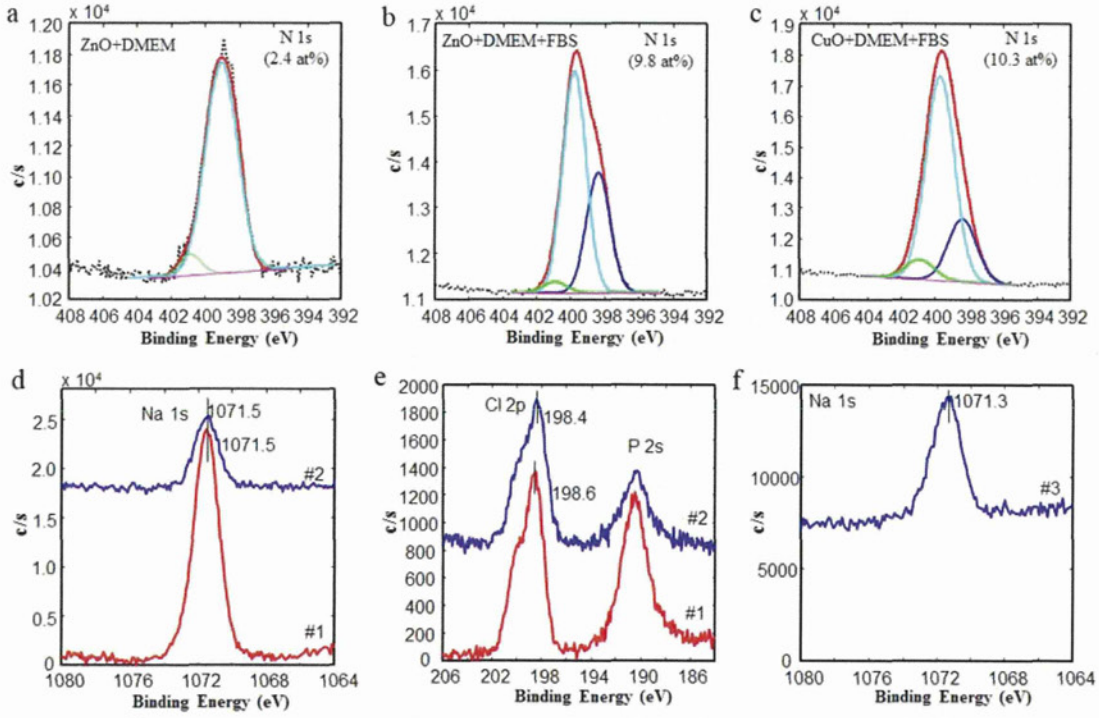

Figure 5 | XPS characterization of selectively bound ions by ZnO and CuO NPs. (a) N1s curve fit of ZnO NPs dispersed in DMEM; (b) N1s curve fit of ZnO NPs dispersed in DMEM with FBS; (c) N1s curve fit of CuO NPs dispersed in DMEM with FBS; (d) Na1s spectra of ZnO NPs dispersed in DMEM (#1) and in DMEM with FBS (#2); (e) Cl2p spectra of ZnO NPs dispersed in DMEM (#1) and in DMEM with FBS (#2); (f) Na1s spectra of CuO NPs dispersed in DMEM with FBS (#3). Compared to the binding energies of the elements of the pristine DMEM and FBS, the binding energy positions in the spectra were shifted.

shown that negatively charged Au NPs are more toxic than positively charged and neutral Au NP counterparts, due to the interaction of the outer Au NP components with cellular components[20]. The interaction of the negatively charged Au NPs with cellular components could in turn influence the mitochondrial membrane potential by releasing positively charged calcium ions from the matrix into the cytosol[20]. Thus, previous work related to the effects of surface charge and surface modification on cell-specific responses and cytotoxicity[21–23] may need to be re-evaluated. That is, the surface may not the one as expected from the intended surface modification. Our finding that NP bio-complexes form in biological environments could be used to help design the NP surfaces for effective drug, DNA and siRAN delivery systems and more accurate nanotoxicity studies.

We did not detect signals from key components of serum proteins, such as N, due to the high energy of the electron beam used in the TEM technique. However, we did observe the disappearance of certain matters during the TEM observation because biomolecules can be easily damaged by high energy beam, which may have been the serum proteins. Previously, Maiorano *et al.* made the assumption that an observed cloud surrounding Au NPs was caused by proteins, based on TEM observations without corresponding elemental maps[24]. Despite this assumption, protein coronas can mediate cellular responses[6] and the toxic effects of NMs[24,25]. We believe that identification of the constituents of NP bio-complexes would significantly improve our understanding of what is selectively acquired by NMs in biological environments; how those acquired constituents influence the reactivity, transport, transformation, bioavailability, and toxicity of NMs; and how the NMs interact with living cells[26,27].

Although there is implication that the binding components from cellular environment had great effects on the toxicity of Au NPs[20], it is currently impossible to describe with certainty all the interactions play at the nano-bio interface in biological environments. The concept of the NP protein corona is important in understanding the dynamic surface properties of NMs in biological fluids. However, even at this moment, it is less clear how the spontaneous formation of a protein corona influences the materials' interactions with biological surfaces and receptors and contributes to biological outcomes of materials. Although it is not surprising that NPs would aggregate in salt rich solutions as this is well known from colloidal theory, the present observation of NMs bio-complexes is certainly new, and such kind of ion corona may be assumed as protein corona if there is no elemental identification[24]. We observed the formation of bio-complexes after naturally drying of the ZnO and CuO NPs immersed in the biological solutions. It remains unclear how dynamically biological environments influence the attaching and detaching of the components from the solution, which is under investigation. Despite challenges to probe events happened at the nano-biointerface, the basic principles of nano-biointerface are being investigated by establishing new imaging techniques, such as TEM and scanning probe microscopy, and biological approaches[5]. The well known colloid chemistry and physics might be considered to be helpful to understand the formation of bio-complexes, however, the behaviors in a biological environment is conceptually different from the well-known colloidal phenomena[6]. By contrast, the methods for protein corona investigation may be extended to explore dynamics of bio-complexes[26,27].

In summary, we have discovered the formation of NM bio-complexes originating from the adsorption of various components in a biological environment onto NMs, independent of proteins. The interaction between NMs and the local environment adds complexity to the challenge of determining the biological outcome of using NMs. Thus, identification of the constituents of these bio-complexes would provide new insights into our understanding of how NMs are modified in biological environments and what cells really see. These results are expected to improve our understanding of the interactions between NMs and live cells. The results of our study are a reminder that our understanding of the nano-bio interactions is still in its infancy.

Methods

Nanoparticles. High-purity ZnO and CuO NPs were obtained from Sigma-Aldrich (Sigma-Aldrich Co., Japan). The primary dimensions and sizes of the oxides were provided in the data sheet, as determined by X-ray diffraction (XRD) and Brunauer–Emmett–Teller (BET) analysis. The average sizes of the ZnO and CuO NPs were 60 nm and 50 nm, respectively, but were not uniform, as previously observed by electron microscopy[16]. In contrast to Au and silica NPs, it is almost impossible to synthesize homogeneous ZnO or CuO NPs with identical shape and size. We characterized the primary size, shape, and composition of the NPs by scanning electron microscopy (SEM) equipped with energy dispersive spectroscopy (EDS) (JSM-7001F, JEOL Inc., Japan) and by X-ray photoelectron spectroscopy (XPS) (PHI Quantera SXM, ULVAC-PHI, Japan)[16]. Note that here we used the averaged primary size as many reports by others[17]. In the regard of varying size of the ZnO and CuO NPs, our observed formation of bio-complex is independent on the size of materials.

Dispersion solvents. DMEM (pH = 7.4) (Invitrogen,) with or without 10% (v/v) FBS (SAFC Bioscience Inc.,) was supplemented with 100 units/mL penicillin and 100 μg/mL streptomycin. The composition of DMEM can be found in the Supplementary Information section. Phosphate buffer saline (PBS) contains $NaHPO_4$, Na_2HPO_4, and NaCl.

Nanoparticle suspension preparation. ZnO and CuO were dispersed in medium with FBS, medium without FBS, PBS, or PBS with FBS. The concentration of the NP suspensions was 25 μg/mL.

TEM characterization. The dark-field TEM images, high-resolution TEM (HRTEM) images, elemental mapping, and EDS were analyzed using a JEM-2100F high-resolution transmission electron microscope (JEOL Inc., Japan) with acceleration voltage of 200 kV. The samples for TEM observation were prepared by immersing TEM mesh into the NP suspension (25 μg/mL) for 24 h at 37°C in the dark with 5% CO_2, the typical cell culture conditions. After naturally drying in air, the TEM mesh was observed.

XPS characterization. PHI Quantera SXM (ULVAC-PHI) with monochromatic Al Kα X-ray (1.5×0.1 mm, 100 W) (pass energy of 55 eV and step of 0.2 eV for narrow spectrum and pass energy of 280 eV and step of 0.5 eV for survey spectrum) was used. Binding energy corrections for the spectra were carried out by using C1s peaks at 285.0 eV. The sample for XPS investigation was prepared by immersing Au substrate into the suspension of NPs in DMEM or DMEM with FBS.

Zeta potential. The surface zeta potentials of the ZnO NPs and CuO NPs were measured by using a laser electrophoresis zeta-potential analyzer (LEZA-600, Otsuka Electronics, Japan). The NPs were dispersed in the solvents with a concentration of 25 μg/mL by sonication for ~60 min to reduce aggregation/agglomeration. The cell unit of the equipment was washed by using the same solvent as that for dispersing NPs prior to measurement. We measured three times for each sample.

1. Chatterjee, D. K., Gnanasammandhan, M. K. & Zhang, Y. Small upconverting fluorescent nanoparticles for biomedical applications. *Small* **6**, 2781–2795 (2010).
2. Kudgus, R. A., Bhattacharya, R. & Mukherjee, P. Cancer nanotechnology: emerging role of gold nanoconjugates. *Anticancer Agents Med. Chem.* **11**, 965–973 (2011).
3. Farokhzad, O. C. & Langer, R. Impact of nanotechnology on drug delivery. *ACS Nano* **3**, 16–20 (2009).
4. Chen, A. M., Taratula, O, Wei, D. G., Yen, H. I., Thomas, T., Thomas, T. J., Minko, T. & He, H. X. Labile catalytic packaging of DNA/siRNA: control of gold nanoparticles "out" of DNA/siRNA complexes. *ACS Nano* **4**, 3679–3688 (2010).
5. Nel, A. E., Mädler, L., Velegol, D., Xia, T., Hoek, E. M. V., Somasundaran, P., Klaessig, F., Castranova, V. & Thompson, M. Understanding biophysicochemical interactions at the nano–bio interface. *Nat. Mater.* **8**, 543–557 (2009).
6. Park, S. & Hamad-Schifferli, K. Nanoscale interfaces to biology. *Curr. Opin. Chem. Biol.* **14**, 616–622 (2010).
7. Keselowsky, B. G., Collard, D. M. & Garcia, A. J. Surface chemistry modulates focal adhesion composition and signaling through changes in integrin binding. *Biomaterials* **25**, 5947–5954 (2004).
8. Cedervall, T., Lynch, I., Lindman, S., Berggard, T., Thulin, E., Nilsson, H., Dawson, K. A. & Linse, S. Understanding the nanoparticle-protein corona using methods to quantify exchange rates and affinities of proteins for nanoparticles. *Proc. Natl. Acad. Sci. U.S.A.* **104**, 2050–2055 (2007).
9. Lunqvist, M., Stigler, J., Elia, G., Lynch, I., Cedervall, T. & Dawson, K. A. Nanoparticle size and surface properties determine the protein corona with possible implications for biological impact. *Proc. Natl. Acad. Sci. U.S.A.* **105**, 14265–14270 (2008).
10. Ehrenberg, M. S., Friedman, A. E., Finkelstein, J. N., Oberdorster, G. & McGrath, J. L. The influence of protein adsorption on nanoparticle association with cultured endothelial cells. *Biomaterials* **30**, 603–610 (2009).

11. Mahmoudi, M., Lynch, I., Ejtehadi, M. R., Monopoli, M. P., Bombelli, F. B. & Laurent, S. Protein-nanoparticle interactions: opportunities and challenges. *Chem. Rev.* **111**, 5610–5637 (2011).
12. Maynard, A. D., Warheit, D. B. & Philbert, M. A. The new toxicology of sophisticated materials: nanotoxicicology and beyond. *Toxicol. Sci.* **120**, S109–S129 (2011).
13. Frug, H. F. & Wick, P. Nanotoxicology: an interdisciplinary challenge. *Angew. Chem. Int. Ed.* **50**, 1260–1278 (2011).
14. Warheit, D. B. Debunking some misconceptions about nanotoxicology. *Nano Lett.* **10**, 4777–4782 (2010).
15. Jiang, J., Oberdörster, G. & Biswas, P. Characterization of size, surface charge, and agglomeration state of nanoparticle dispersions for toxicological studies. *J. Nanopart. Res.* **11**, 77–89 (2009).
16. Xu, M. S., Fujita, D., Kajiwara, S., Minowa, T., Li, X. L., Takemura, T., Iwai, H. & Hanagata, N. Contribution of physicochemical characteristics of nano-oxides to cytotoxicity. *Biomaterials* **31**, 8022–8031 (2010).
17. Xia, T., Kovochich, M., Liong, M., Madler, L., Gilbert, B., Shi, H., Yeh, J. I., Zink, J. I. & Nel, A. E. Comparison of the mechanism of toxicity of zinc oxide and cerium oxide nanoparticles based on dissolution and oxidative stress properties. *ACS Nano* **2**, 2121–2134 (2008).
18. Villanueva, A., Canete, M., Roca, A. G., Calero, M., Veintemillas-Verdaguer, S., Serna, C. J., Morales, M. D. & Miranda, R. The influence of surface functionalization on the enhanced internalization of magnetic nanoparticles in cancer cells. *Nanotechnology* **20**, 115103 (2009).
19. Verma, A. & Stellacci, F. Effect of surface properties on nanoparticle-cell interactions. *Small* **6**, 12–21 (2010).
20. Schaeublin, N. M., Braydich-Stolle, L. K., Schrand, A. M., Miller, J. M., Hutchison, J., Schlager, J. J. & Hussain, S. M. Surface charge of gold nanoparticles mediates mechanism of toxicity. *Nanoscale* **3**, 410–420 (2011).
21. Asati, A., Santra, S., Kaittanis, C. & Perez, J. M. Surface-charge-dependent cell localization and cytotoxicity of cerium oxide nanoparticles. *ACS Nano* **4**, 5321–5331 (2010).
22. Bhattacharjee, S., de Haan, L. H. J., Evers, N. M., Jiang, X., Marcelis, A. T. M., Zuilhof, H., Rietjens, I. M. C. M. & Alink, G. M. Role of surface charge and oxidative stress in cytotoxicity of organic monolayer-coated silicon nanoparticles towards macrophage NR8383 cells. *Particle Fibre Toxicol.* **7**, 25 (2010).
23. Thevenot, P., Cho, J., Wavhal, D., Timmons, R. B. & Tang, L. Surface chemistry influences cancer killing effect of TiO_2 nanoparticles. *Nanomed.* **4**, 226–236 (2008).
24. Maiorano, G., Sabella, S., Sorce, B., Brunetti, V., Malvindi, M. A., Cingolani, R. & Pompa, P. P. Effects of cell culture media on the dynamic formation of protein–nanoparticle bio-conjugates and influence on the cellular response. *ACS Nano* **4**, 7481–7491 (2010).
25. Hu, W., Peng, C., Lv, M., Li, X., Zhang, Y., Chen, N., Fan, C. & Huang, Q. Protein corona-mediated mitigation of cytotoxicity of graphene oxide. *ACS Nano* **5**, 3693–3700 (2011).
26. Casals, E., Pfaller, T., Duschl, A., Oostingh, G. J. & Puntes, V. Time evolution of the nanoparticle protein corona. *ACS Nano* **4**, 3623–3632 (2010).
27. Walczyk, D., Bombelli, F. B., Monopoli, M. P., Lynch, I. & Dawson, K. A. What the cell "sees" in bionanoscience, *J. Am. Chem. Soc.* **132**, 5761–5768 (2010).

Acknowledgements

This work was partially supported by the National Natural Science Foundation of China (Nos. 51011130028, 50990063 and 50973095), by Zhejiang Provincial Natural Science Foundation of China (Youth Talent Program: R4110030), Science and Technology Department of Zhejiang Provincial (Qianjiang Talent Program: 2011R10077), the Fundamental Research Funds for the Central Universities of China (No.: 2011QNA4030), and by the Interdisciplinary Laboratory for Nanoscale Science and Technology & Material Analysis Station, National Institute for Materials Science (NIMS), Japan. We thank Y. Nemoto and H. Gao for assistance with TEM measurements.

Author contributions

M.S.X. originated the work and designed the experiments. M.S.X. performed the experiments, analyzed the data and prepared the manuscript. J.L. and N.H. performed zeta potential experiments. H.I. performed XPS measurement and data analysis. Q.S.M. carried out XRD measurement and data analysis. All discussed the results.

Additional information

Supplementary information accompanies this paper at http://www.nature.com/scientificreports

Competing financial interests: The authors declare no competing financial interests.

How to cite this article: Xu, M. *et al.* Formation of Nano-Bio-Complex as Nanomaterials Dispersed in a Biological Solution for Understanding Nanobiological Interactions. *Sci. Rep.* **2**, 406; DOI:10.1038/srep00406 (2012).

JOURNAL OF NANOBIOTECHNOLOGY

RESEARCH Open Access

Genotoxicity and molecular response of silver nanoparticle (NP)-based hydrogel

Liming Xu[1,2*], Xuefei Li[2], Taro Takemura[3], Nobutaka Hanagata[3], Gang Wu[2] and Laisheng Lee Chou[4*]

Abstract

Background: Since silver-nanoparticles (NPs) possess an antibacterial activity, they were commonly used in medical products and devices, food storage materials, cosmetics, various health care products, and industrial products. Various silver-NP based medical devices are available for clinical uses, such as silver-NP based dressing and silver-NP based hydrogel (silver-NP-hydrogel) for medical applications. Although the previous data have suggested silver-NPs induced toxicity in vivo and in vitro, there is lack information about the mechanisms of biological response and potential toxicity of silver-NP-hydrogel.

Methods: In this study, the genotoxicity of silver-NP-hydrogel was assayed using cytokinesis-block micronucleus (CBMN). The molecular response was studied using DNA microarray and GO pathway analysis.

Results and discussion: The results of global gene expression analysis in HeLa cells showed that thousands of genes were up- or down-regulated at 48 h of silver-NP-hydrogel exposure. Further GO pathway analysis suggested that fourteen theoretical activating signaling pathways were attributed to up-regulated genes; and three signal pathways were attributed to down-regulated genes. It was discussed that the cells protect themselves against silver NP-mediated toxicity through up-regulating metallothionein genes and anti-oxidative stress genes. The changes in DNA damage, apoptosis and mitosis pathway were closely related to silver-NP-induced cytotoxicity and chromosome damage. The down-regulation of CDC14A via mitosis pathway might play a role in potential genotoxicity induced by silver-NPs.

Conclusions: The silver-NP-hydrogel induced micronuclei formation in cellular level and broad spectrum molecular responses in gene expression level. The results of signal pathway analysis suggested that the balances between anti-ROS response and DNA damage, chromosome instability, mitosis inhibition might play important roles in silver-NP induced toxicity. The inflammatory factors were likely involved in silver-NP-hydrogel complex-induced toxic effects via JAK-STAT signal transduction pathway and immune response pathway. These biological responses eventually decide the future of the cells, survival or apoptosis.

Keywords: Silver nanoparticle-based hydrogel (silver-NP-hydrogel), Genotoxicity, Global gene expression, DNA damage, Apoptosis and mitosis pathway, JAK-STAT signal transduction pathway

Background

Since the 2000s with the development of nanotechnology, various nanomaterials have been commercially used in a wide range of areas. Due to their antibacterial activity, silver-nanoparticles (NPs) are used commonly in medical products and devices, food storage materials, cosmetics, various health care products, and industrial products. In medical applications, silver-NPs have been used for silver-based dressings [1,2], silver-coated catheters [3,4], silver-based hydrogel [5-7]. Silver-NP-hydrogel composites are composed of silver-NP and hydrogel which are used as carrier for silver particles. Most studies focused on manufacturing methods and antibacterial activity of silver-NP-hydrogel composites [5-7].

In recent years, increasing data demonstrated that silver-NPs could induce toxicity in vivo under a variety of exposure conditions including inhalation [8-10], orally [11,12] and via hypodermic injection [13]. Some in vitro studies revealed that silver-NPs could cause strong cytotoxicity in a broad spectrum of cells [14-25], such as germline stem cells

* Correspondence: xuliming@nifdc.org.cn; Lchou@bu.edu
[1]Institute for Medical Devices Control, National Institutes for Food and Drug Control (NIFDC), No. 2 Temple of Heaven, Beijing 100050, China
[4]Goldman School of Dental Medicine, Boston University, 801 Albany Street, Suite 200, Boston, MA 02118-2392, USA
Full list of author information is available at the end of the article

[15], messenchymal stem cells (hMSCs) [16-18], BRL 3A rat liver cells [19], NIH3T3 cells [20], HepG2 human hepatoma cells [21], normal human lung fibroblasts (IMR-90), human glioblastoma cells (U251) [22,23], human normal bronchial epithelial (BEAS-2B) cells [24] and HeLa cells [25]. Many studies also reported that silver-NPs induced potential genotoxicity in several types of cells [21-24,26]. With the concerns about the safety and clinical risks associated with silver-NP-based medical products, however, a little is know about the molecular mechanism of silver-NP induced toxicity.

Metal ions including silver act as catalysts and can produce reactive oxygen species (ROS) in the presence of oxygen, which is considered to be a mechanism of toxicity and genotoxicity for metal nanomaterials. Acting as signal molecules, ROS, can promote cell cycle progression and induce oxidative DNA damage [19,27-29]. CBMN assay [30] is sensitive to ROS-mediated DNA damage, making it suitable for assessing the genotoxicity potentially induced by nanomaterials. Therefore, CBMN assay was selected to assess genotoxicity of silver-NP-hydrogel in this study.

Technique of microarray provides a way of studying biocompatibility of biomaterials at molecular level [31]. The global gene expression analysis using the microarray technique could gain profiling information of nanomaterial-cell interactions [25,32,33].

In this study, in vitro genotoxicity and molecular responses of silver-NP-hydrogel were assessed by CBMN assay and global gene expression analysis. The results provided scientific evidence for understanding the biosafety and potential clinical risk of silver-NP-based products.

Results

Genotoxicity

To know whether silver-NP-hydrogel has potential genetoxicity, a CBMN assay was conducted for assessing chromosome damage by silver-NP-hydrogel in HeLa cell cultures. The results were presented as the frequency of micronucleation per 1000 BNCs (Table 1). The MMC treatment (positive control) showed a MNF of 20.6% ± 2.47, showing a significant difference compared to the NaCl solution treatment (negative control), which had a MNF of 2.5% ± 0.79 ($P < 0.05$). It confirmed that the test system worked well. There was a significant increase in the MN frequency at 20 mg/ml ($P < 0.05$), 40 mg/ml ($P < 0.05$) and 60 mg/ml ($P < 0.05$) of silver-NP-hydrogel exposure, this was not observed at the hydrogel treatment alone ($P = 0.116$). These results suggested that the silver-NP-hydrogel induced chromosome damage in HeLa cells.

Cellular response at molecular levels

To assess the cellular response induced by silver-NP-hydrogel exposure at the molecular level and the mechanisms of toxic effects, global gene expression and GO pathway analysis was performed using the DNA microarray technique. The graphical abstract of working process for global gene expression analysis was shown in Figure 1.

Table 1 The CBMN assay of HeLa cells post-exposed to silver-NP-hydrogel and hydrogel for 24 h

Test	Dose	FMN (%)	95% Confidence Interval for mean Lower Bound	Upper Bound
NC (NaCl sol.)	50 μl	2.5 ± 0.79	5.3	44.7
Hydrogel	60 mg/ml	3.7 ± 0.66	20.7	53.3
Silver-NP Gel	20 mg/ml	7.0 ± 0.82*	49.7	90.3
	40 mg/ml	8.67 ± 0.32*	78.7	94.7
	60 mg/ml	9.47 ± 0.3*	87.6	102.5
PC (MMC)	0.05 μg/ml	20.6 ± 24.7*		

Mitomycin C (MMC) was used as a positive control (PC). NaCl solution (NaCl sol.) was used as a negative control (NC). The results were presented as percentage of micronucleation frequency (FMN %) in 1000 binucleation cells. The significance of positive control compared to negative control was identified using *T*-Test. The significance of all test samples compared to negative control was identified using ANOVA and Dunnett tests (2-sided).
*, $P < 0.05$. The data indicate the mean ± SD (n = 3).

The morphological changes of cells

After exposing cells to 40 mg/ml silver-NP-hydrogel (contained 15.2 μg of silver-NPs) for 24 h and 48 h, the cells lost their normal epithelial cell morphology, becoming longer, and swelled. In contrast, cells exposed to hydrogel (without silver-NPs) did not show significant difference compared to the non-treatment control (Figure 2).

Gene expression profiling

According to the defined filtering criteria as described in "Materials and methods", the differentially expressed genes in both silver-NP-hydrogel and hydrogel alone groups, including up-regulated and down-regulated genes, are shown in Additional files 1, 2, 3, 4, 5, 6, 7 and 8. A total of 1,258 genes (Additional file 1) were up-regulated and 788 genes (Additional file 2) were down-regulated at 24 h exposure to silver-NP-hydrogel. Also, 1,532 genes (Additional file 5) were up-regulated and 824 genes (Additional file 6) were down-regulated at 24 h exposure to hydrogel alone. After the 48 h exposure, a total of 843 genes (Additional file 3) were up-regulated and 642 genes (Additional file 4) were down-regulated from silver-NP-hydrogel exposure. In contrast, 99 genes (Additional file 7) were up-regulated and 370 genes (Additional file 8) were down-regulated from exposure to hydrogel alone.

By comparing 24 h and 48 h gene expression profiling, it was observed that the 21.7% of genes that were up-regulated at 24 h post-exposure to silver-NP-hydrogel were continuously highly expressed until the 48 h exposure (273 genes, Additional file 9) (Figure 3A). This suggested that the silver-NP-hydrogel continuously induced gene up-regulation at 48 h exposure. In addition, 19.16% of the genes that were down-regulated at 24 h post-exposure, were

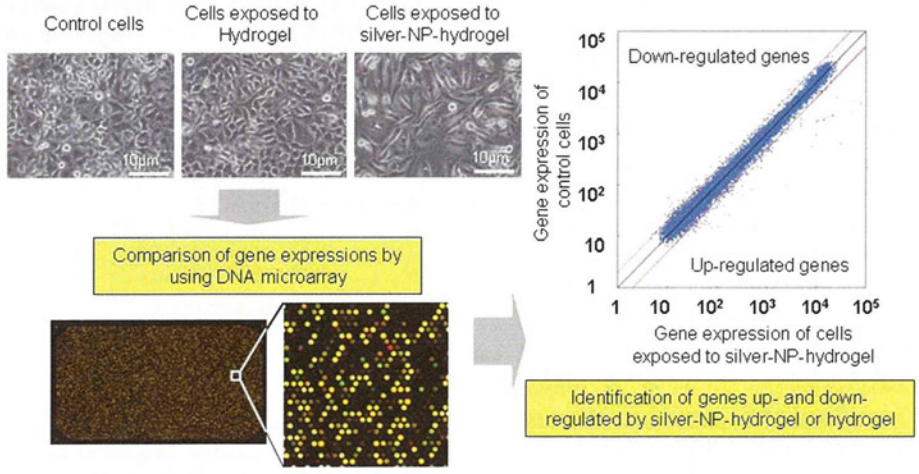

Figure 1 The graphical abstract of working process for global gene expression analysis. After exposure to silver-NP-hydrogel and Hydrogel, the treated cells and non-treatment control cells were harvested. Gene expression profiling was analysis by DNA microarray technique. The differential expressed genes were identified by comparing the gene expression levels in treated cells with that in the control cells without treatment.

continuously lower-expressed until the 48 h exposure (151 genes, Additional file 10) (Figure 3A). This suggested that the silver-NP-hydrogel continuously caused gene down-regulation at the 48 h exposure period.

In contrast, most of the up-regulated genes at 24 h exposure to hydrogel alone had recovered after continuous exposure up to 48 h. Only 1.76% of up-regulated genes at 24 h exposure continuously showed higher-expression at 48 h (27 genes, Additional file 11) (Figure 3B). This observation suggested that the gene up-regulation was a transient response in the cells against the extracellular stimulation from the hydrogel. However, 16.75% of genes that were down-regulated at 24 h post-exposure to hydrogel alone, were continuously lower-expressed until 48 h exposure (138 genes, Additional file 12) (Figure 3B). These results suggested that down-regulated genes rather than up-regulated genes might play a role in the cell response against hydrogel alone.

By further comparing changed genes common to both silver-NP-hydrogel and hydrogel alone exposure, it was found that, of the 843 up-regulated genes at 48 h silver-NP-hydrogel exposure, only 3.91% of genes were common to those expressed at hydrogel alone exposure (33 genes, Additional file 13); and 96.09% of the genes were unique for silver-NP-hydrogel exposure (Figure 3C). For the 642 down-regulated genes at 48 h of silver-NP-

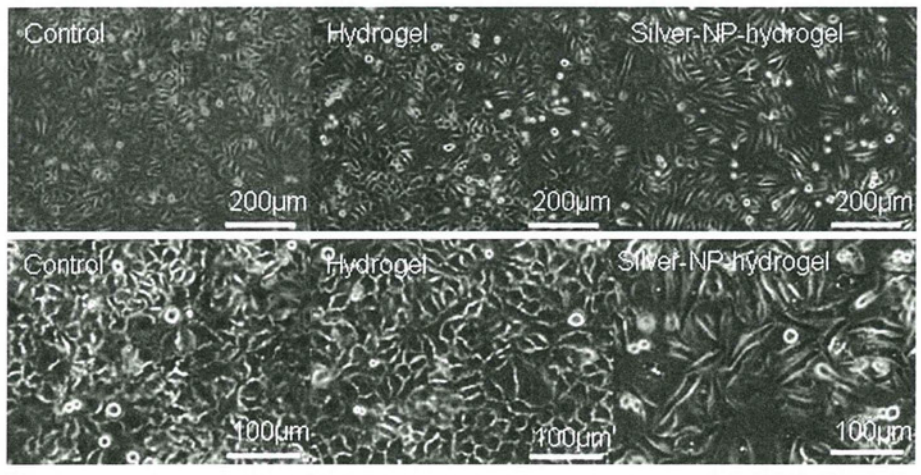

Figure 2 Cell morphological changes. The cells were post-exposed with silver-NP-hydrogel (40 mg/ml) and Hydrogel (40 mg/ml) as the study groups and with no treatment as a control for 24 h (up-panel, X 200) and 48 h (bottom-panel, X 400). The changes of cell morphology were visualized by light microscopy.

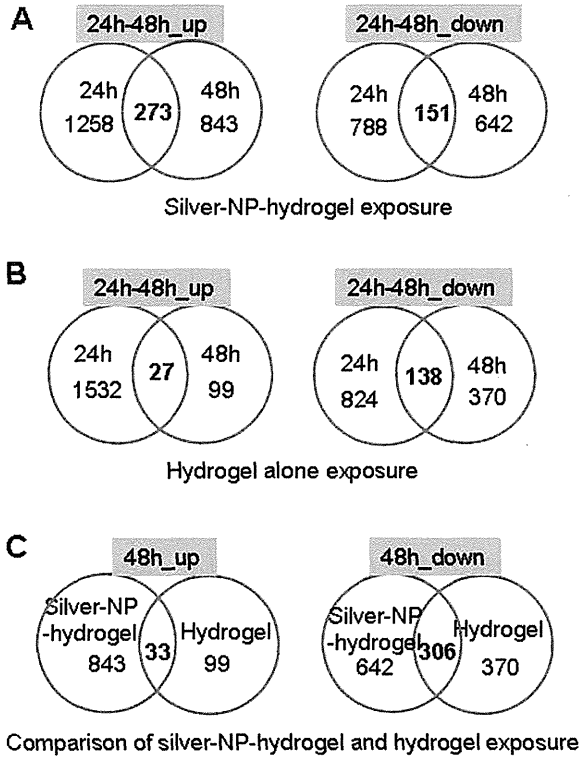

Figure 3 Gene expression profiling based on DNA microarray data. A, Up- and down-regulated genes in silver-NP-hydrogel exposed HeLa cells (Additional file 1, 2, 3 and 4); B, Up- and down-regulated genes in hydrogel alone exposed HeLa cells (Additional file 5, 6, 7 and 8); C, A comparison of common expressed genes in the silver-NP-hydrogel and hydrogel alone exposed cells (Additional file 13 and Additional file 14).

hydrogel exposure, 46.66% (306 genes, Additional file 14) of genes were common to those expressed at hydrogel alone exposure; and 53.34% of the genes were unique changes for silver-NP-hydrogel exposure (Figure 3C). These results suggested that the up-regulated genes induced by silver-NP-hydrogel could be mainly attributed to silver-NPs and that the down-regulated genes induced by silver-NP-hydrogel could be attributed in part to silver-NP and hydrogel components. It was indicated that silver-NPs could play a key role in the silver-NP-hydrogel induced toxicity, while hydrogel components might also play a role in the toxic response to silver-NP-hydrogel by down-regulating some gene expressions.

GO function analysis of differential expressed genes

Based on gene ontology (GO) biological processes, the genes which were up- and down-regulated at 48 h of silver-NP-hydrogel exposure were further analyzed using the program of GO Surfer. With the gene number-based signal pathway activation analysis, the GO pathway which has theoretically significant activation ($p < 1.0E-03$) was further picked-up as shown in Table 2 and Table 3.

Pathway analysis of GO/Biological processes showed that fourteen functional signal pathways were related to up-regulated genes at 48 h of silver-NP-hydrogel exposure (Table 2), suggesting that the up-regulated genes might play an important role in adverse cell responses. These fourteen functional signal pathways were unique for silver-NP-hydrogel exposed cells, but not common to hydrogel alone exposed cells, suggesting that the changes in functional signal pathways were attributed to silver-NPs. Under the same analysis method, in contrast, non-signal pathway which was theoretical significant activation was observed in up-regulated genes at 48 h of hydrogel alone exposure (data not shown). In addition, the most up-regulated genes at 24 h exposure had recovered at 48 h of hydrogel exposure (Figure 3B). It was further suggested that the up-regulated genes induced by the hydrogel components might not affect cell function. Several pathways were related to down-regulated genes at 48 h of silver-NP-hydrogel exposure (Table 3). These included the nucleobase, nucleoside, nucleotide and nucleic acid metabolic processes pathway, cell cycle pathway and mitosis pathway. These results suggested that the down-regulated genes might cause cell damage by affecting cell proliferation, cell cycles and mitosis. The later two pathways, being unique to silver-NP-hydrogel exposure, were not common to hydrogel alone exposure, suggesting that the changes of these functional signal pathways are mainly

Table 2 GO function analysis of differential expressed genes at 48 h exposure of silver-NP-hydrogel

Functional GO pathway	REF.-LIST*/Up-exp#/expected$	P value
cell communication	4365/231/174.28	p = 1.04E-06
cell-cell signaling	1331/81/53.14	p = 2.14E-04
cell adhesion	1333/77/53.22	p = 8.67E-04
signal transduction	4191/215/167.34	p = 2.37E-05
intracellular signaling cascade (JAK-STAT cascade)	1568/102/62.61	p = 1.02E-06
metabolic process	8267/373/330.08	p = 7.32E-04
lipid metabolic process	1119/94/44.68	p = 7.32E-12
carbohydrate metabolic process	952/69/38.01	p = 1.08E-06
response to stimulus	1798/119/71.79	p = 7.96E-08
transport	2857/164/114.07	p = 6.18E-07
endocytosis	575/43/22.96	p = 9.23E-05
cellular defense response	457/38/18.25	p = 2.75E-05
immune system process	2628/171/104.93	p = 7.69E-11
immune response	756/52/30.19	p = 1.41E-04

* reference list, that is all genes number related to the GO pathway;
# up-expressed genes number in this study;
$ expected minimum genes number for activating of signal pathway.
Based on the gene ontology (GO) biological process, the GO pathway, which has theoretically significant activation ($p < 1.0E-03$), related to up-regulated genes.

Table 3 GO function analysis of differential expressed genes at 48 h exposure of silver-NP-hydrogel

Functional GO pathway	REF.-LIST*/Down-exp#/expected$	P value
nucleobase, nucleoside, nucleotide and nucleic acid metabolic processes	3825/138/81.84	p = 8.40E-12
cell cycle	1840/62/39.37	p = 2.60E-04
mitosis	635/27/13.59	p = 6.90E-04

* reference list, that is all genes number related to the GO pathway;
# down-expressed genes number in this study;
$ expected minimum genes number for activating of signal pathway.
Based on the gene ontology (GO) biological process, the GO pathway, which has theoretically significant activation ($p < 1.0E-03$), related to down-regulated genes.

attributed to silver-NPs. These events were considered to be closely involved with cytotoxicity and genotoxicity. At 48 h of hydrogel exposure, three pathways related to down-regulated genes were also showed theoretical significant activation. They included a metabolic process (p = 4.02E-04), nucleobase, nucleoside, nucleotide and nucleic acid metabolic processes (p = 1.69E-10) and the primary metabolic process (p = 2.97E-04). These results suggested that the down-regulated genes induced by hydrogel alone might have some effect on cell proliferation and metabolism.

Real-time PCR verification of differential expressed genes

To verify the reliability of differential expressed gene identified by the DNA microarray, five genes selected from up- and down-regulated genes expressed in silver-NP-hydrogel 48 h exposure were further examined with real-time PCR detection. The results showed that the gene expression was basically consistent with that of the microarray analysis, indicating a good reliability and reproducibility of the microarray in the current study (Table 4).

Discussion

Genotoxicity evaluation is an idea assessment of biosafety at molecular level for nanomaterials-based medical devices. In this study, a significant increases in the micronucleation frequency (MNF) of HeLa cells was induced by the silver-NP-hydrogel exposure at concentrations of 20-, 40-, and 60-mg/ml (in medium), compared to the negative control ($P < 0.05$), suggesting that the silver-NP-hydrogel has a potential risk of genotoxicity. The study also showed that hydrogel alone did not show significant change, compared to the negative control, suggesting that genotoxicity caused by silver-NP-hydrogel was attributed to silver-NPs. Kawata et al. demonstrated that exposure to 1.0 μg/ml of silver-NPs (7–10 nm in size) induced MNF up to 47.9% in the HepG2 cell line [21]. AshaRani et al. reported that exposure at the 25 μg/ml of silver-NPs (6–20 nm in size) induced chromosomal aberrations in 10% of the IMR-90 normal cell line, and in 20% of the U251 cancer cell line [22,23]. In the comet assay and micronucleus (MN) assay for BEAS-2B cells, silver-NPs (43–260 nm in size, dispersed in medium) stimulated DNA breakage and MN formation in a dose-dependent manner [24]. In this study, the size of silver nanoparticles contained in silver-NP-hydrogel ranged from 5 nm to 30 nm (observed by TEM, dispersed in water). Number of studies has reported for the in vivo genotoxicity and carcinogenicity by silver-NPs. Study by Kim et al. reported that there was no genotoxic effect in rats after 28 days oral exposure to Ag NPs [11]. Kim et al. also reported that no genotoxic effect in rats after 90 days inhalation of Ag NPs [34]. In contrast, however, our recent study reported that silver-NP-hydrogel induced micronuclei, nuclei disruption, chromatin concentration and cell apoptosis in rabbit reproductive organ tissues in silver-NP-hydrogel administration through the vagina [35]. The difference of findings in potential genotoxic and carcinogenic risks of nanomaterials is possibly due to the insufficient characterization of test material, difference in the experimental design, use of different animal models and species, difference in dosimetry, and different targeting organs [36]. It was known that confirmation of asbestos nanofiber as a carcinogen in Japan took over 10 years [37]. Since the silver nanoparticles are still widely used clinically in some countries, it is important to gain a better understanding of their genotoxicity and carcinogenecity.

Table 4 The gene expression detected by real-time PCR and detected by DNA microarray at 48 h exposure of silver-NP-hydrogel

determination	IL1A	HMOX1	DDIT3	MT1F	PDGFRB
Real-time PCR ($2^{-\nabla\nabla Ct}$)	15.97	6.58	8.18	82.96	0.4
DNA microarray (fold changes)	2.76	2.41	2.17	5.63	−2.14

Two important molecular mechanisms were considered to be involved in the in vitro toxicity and genotoxicity induced by silver-NP-hydrogel, as further discussed below.

The balance between anti-ROS-toxicity and DNA damage

From the data in this study, the signaling pathways and regulatory proteins involved in anti-ROS-toxicity, DNA damage, apoptosis, cell cycles and mitosis might be associated with genotoxicity caused by silver-NP-hydrogel.

Metallothioneins (MTs) are considered to be essential biomarkers in metal-induced toxicity [38] as facilitating metal detoxification and protection from free radicals [39]. A report on heavy metal toxicity in Javanese medaka showed that MT upregulation occurs in silver mediated toxicity [40]. Hemeoxygenase-1 (HO-1) is an ROS sensor and a cryoprotective agent possessing antioxidant and anti-inflammatory properties. HO-1 breaks down heme to antioxidant biliverdin, carbon monoxide and iron under stress conditions [41,42]. It was reported that oxidative stress response genes (superoxide dismutase 2, glutathione reductase 1, etc.) in mouse brain following silver-NP exposure were upregulated [43]. In the present study, 10 metal-

lothionein genes (MT1F, MT1A, MT2A, MT1B, MT1G, MT1H, MT1X, MT1L, MT1M, MT1E), HO-1 and oxidative stress induced growth inhibitor 1 (OSGIN1) were significantly up-regulated at 48 h of silver-NP-hydrogel exposure [Additional file 5 and Additional file 6]. All these molecules are believed to protect cells against metal-induced ROS toxicity. Metal ions including silver act as catalysts and can produce reactive oxygen species in the presence of oxygen, which is thought to be a mechanism of toxicity. Previous studies showed that silver-NPs increase the production of intracellular ROS [20]. The ROS can act as signal molecules promoting cell cycle progression, and can induce oxidative DNA damage [27-29]. We previously reported that HeLa cells exposed to silver-NPs consistently over-express isoforms of metallothionein (MT1A, MT1F, MT1G, MT1X, and MT2A) [25]. AshaRani et al. reported that the MT-1 F and HO-1 were upregulated in IMR-90 cells following silver-NP treatment [22]. Kawata et al. also reported that three metallothionein genes (MT1H, MT1X, MT2A) were significantly upregulated in HepG2 cells exposed to silver-NPs [21]. These studies suggested that the cells protect themselves against silver NP-mediated toxicity through up-regulating metallothionein genes and oxidative stress induced genes.

On the other hand, the genes which are related to the DNA damage and apoptosis, such as DNA-damage-inducible transcript 3 (DDIT3), caspase 1, and apoptosis-related cysteine peptidase (CASP1) were up-regulated by silver NPs. Changes in chromosome related genes (24 genes up-regulated and 26 genes down-regulated) (Additional file 3 and Additional file 4) found in this study might damage the chromosomes. Apoptosis inhibitors, such as BCL2 interacting protein (HRK), BIK (BCL2-interacting killer, apoptosis-inducing), Fas apoptotic inhibitory, molecule 3 (FAIM3), apoptosis inhibitor (FKSG2), suppression of tumorigenicity 13 (ST13), growth arrest and DNA-damage-inducible, alpha (GADD45A) were also significantly up-regulated. This suggested that silver nanoparticles induced apoptosis via a mitochondrial pathway. Apoptosis and chromosome damage could be subsequently involved in cytotoxicity and genotoxicity.

In addition, analysis of the activating signal pathways in this study also suggested that cell cycles and the mitosis signal pathway were significantly down-regulated, which was uniquely represented at the silver-NP-hydrogel 48 h exposure. These pathways are considered to be closely involved in cell proliferation, apoptosis and tumorigenesis progression. There were 62 genes related to cell cycle signal pathways. Among them, 27 genes were related to mitosis pathway (Additional file 15). In these genes, cell division cycle 14 homolog A (CDC14A) showed a 13 -fold ($\log_2 = -3.71$) down-regulation. CDC14A is a member of the dual specificity protein tyrosine phosphatase family. It is highly similar to saccharomyces cerevisiae Cdc14, a protein tyrosine phosphatase involved in the exit of cell mitosis and initiation of DNA replication, playing a role in cell cycle control. CDC14A protein has been shown to interact with and dephosphorylate the tumor suppressor protein p53, and is thought to regulate the function of p53 [44]. Human CDC14A shares sequence similarity with the recently identified tumor suppressor, MMAC1/PTEN/TEP1. CDC14A is located at chromosome band 1p21, a region that has been shown to exhibit loss of heterozygosity in highly differentiated breast carcinoma and malignant mesothelioma. Thus, CDC14A has been thought to be a tumor suppressor gene [44]. The down-regulation of CDC14A in this study suggested that it might play a role in the potential genotoxicity induced by silver-NP-hydrogel.

As summarized in Figure 4, the balance between anti-ROS-toxicity and DNA damage, apoptosis, mitosis inhibition of the cells could be the main events which decide the future of the cells.

JAK-STAT signal transduction pathway

The JAK-STAT (Janus kinase/signal transducers and activators of transcription) cascade is an important signal pathway which affects basic cell functions such as cell growth, differentiation and apoptosis [45]. STAT is a signal transducer and activator of transcription. It conveys or transduces the signal from the receptor-JAK (Janus Kinase) complex to the DNA in the cell nucleus [45]. In mammals, the JAK-STAT signal pathway is the principal signaling mechanism for a wide array of cytokines and growth factors [45,46]. Defects in JAK-STAT proteins can result in immune deficiency disease and cancer [45]. JAKs, which have tyrosine kinase activity, bind to some cell surface cytokine receptors. So, the cytokines, as ligands, through binding to the receptor would trigger activation of JAKs [46-50]. In this

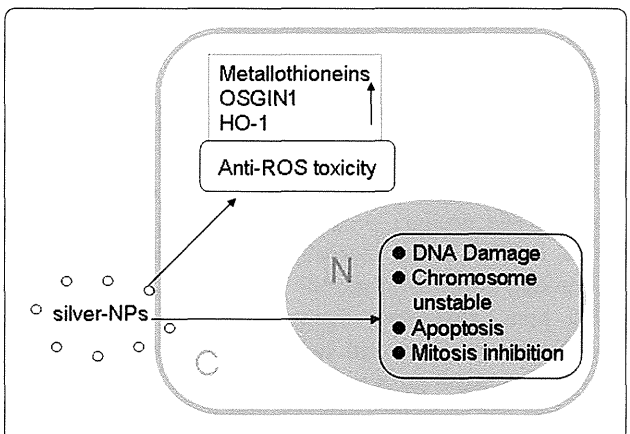

Figure 4 Scheme of molecular mechanisms of cellular response against silver-NP-hydrogel exposed. The balance among anti-ROS-toxicity and DNA damage, apoptosis, mitosis inhibition of the cells might play important role in cytotoxicity. These responses were mainly induced by silver-NPs contained in silver-NP-hydrogel.

study, it was found that silver-NP-hydrogel exposure induced JAK-STAT cascade-related gene up-regulation, not only at 24 h exposure but also for 48 h exposure [Additional file 5 and Additional file 6], and implied that the silver-NP-hydrogel might play a role in JAK-STAT pathway.

It was found by further analysis that many interferon-induced proteins (IFI), interferon-induced protein in the tetratricopeptide (IFIT) family, and interleukin (IL) family were up-regulated (Additional file 5 and Additional file 6). These inflammatory factors acting as ligands while they participate in immune response pathway, may also trigger the activation of JAK-STAT signal pathway through binding to the JAK receptor.

Conclusions

In summary, the silver-NP-hydrogel induced micronuleus formation in HeLa cells. The toxic effects caused by silver-NP-hydrogel arrived mainly from silver-NPs. Based on DNA microarray and GO pathway analysis, the molecular response and mechanisms of toxicity induced by silver-NP-hydrogel might relate to some up-regulated genes involved in fourteen theoretical activating signaling pathways and to some down-regulated genes involved in three signal pathways at 48 h of silver-NP-hydrogel exposure in HeLa cells. These signal pathways play important roles in metabolisms, cell communication, signal transduction, cellular defense response, transport, cell cycles and mitosis. The down-regulation of CDC14A via mitosis pathway suggested that it may play a role in the potential genotoxicity induced by silver-NP. The balances between anti-ROS response and DNA damage, chromosome instability and mitosis inhibition might play important roles in silver-NP induced toxicity. It was also demonstrated that activations of both JAK-STAT signal transduction pathway and immune response pathway could be involved in the mechanisms of toxicity caused by silver-NP-hydrogel.

Materials and methods

Test materials and chemicals

Silver-NP-based hydrogel (silver-NP-hydrogel) used in this study was a clinical available product, and has been used in clinic for treating cervicitis and cervical erosion of women. The product provided by Egeta Co. (Shenzhen, China, Batch Number 090701) was manufactured by simply mixing aqueous silver-NP solution (concentration of 2,000 ppm, purchased from Nanux, Korea, Cat. No. SL1105001) and hydrogel components to achieve a concentration of 0.38 μg/mg (silver- NP-hydrogel). The silver NPs were not coated by any compounds such as PVP, citrate or BSA. To determine the NP size distribution, silver-NP-hydrogel was dissolved in water. Then, the silver particles were collected by centrifuging and placed on a cuppernet for evaluation of size distribution by TEM (Additional file 16: Figure S1). As determined through TEM, the size distribution of the nanoparticles was as follows: 3–5 nm, 47.9%; 5–10 nm, 50.8%; 10–30 nm, 1.3%. The hydrogel was composed of sterile water, glycerine, carbomer and triethanolamine (TEA). The hydrogel component alone (without silver-NP) was used as the compared control.

Cytochalasin B (Cyt-B), Mitomycin C (MMC) and Dimethyl sulfoxide (DMSO) were purchased from Sigma-Aldrich (USA). The Cyt-B was dissolved in DMSO (2.0 mg/ml), and the MMC was dissolved in NaCl solution (10 μg/ml) for use as a stock solution. All solutions were sterilized by using 0.2 μm-pore film and stored at −20°C.

Cell culture and treatment

Silver-NP-hydrogel is currently a clinical product on the markets and is commonly used for treating cervicitis and cervical erosion of women. Therefore, the HeLa cell line was chosen as a cell model in this study. HeLa cells were originally purchased from RIKEN (Wako, Japan) with a RIKEN Cell line number. RCB0007. The cells were cultured in DMEM (GIBCO, USA), with 10% FBS (GIBCO, USA) and 100 U/ml penicillin/100 μg/ml streptomycin (GIBCO, USA), in a humidified 5% CO_2 atmosphere at 37°C.

To determine a suitable concentration of silver-NP-hydrogel for the study, a preliminary experiment was performed by adding silver-NP-hydrogel to culture medium at concentrations of 2.5, 5, 10, 20, 40, and 60 mg/ml. After ultrasonic treatment (300 W, 42 kHz,) for 10 min, the media with various concentrations of silver-NP-hydrogel was applied to cells which had been pre-cultured for 24 h (70–80% confluence), and the cells were then cultured for another 24 h. Cell viability was determined using a methyl tetrazolium (MTT) assay by measuring the optical density of the formazan product. Briefly, after the exposure to silver-NP-hydrogel solution, the cells were washed. A mixture of 20 μl of MTT (5 mg/ml) and 100 μl of non-phenol-red medium were added to the cells, and incubated for 4 h. After through washes and DMSO treatment, 100 μl of the supernatant of each sample was transferred for optical density (OD) detection. The assay was performed using a plate reader at a wavelength 570 nm, with 630 nm as the reference wavelength. The results represented a percentage of the relative viability of cells against to the untreated control. Based on this preliminary experiment, a middle-level viability inhibition of the cells, compared to that in the non-treatment control cells, was found at a concentration (IC50) about 40 mg/ml of silver-NP-hydrogel (in culture media) which containing 15.2 μg/ml of silver-NPs. This concentration was determined according to the concentration-relative cell viability (%) curve equation, and the non-treatment control cell viability (OD level) was served as 100%. An EC50 NP concentration was selected also because the EC50 or IC50 is a conventional coefficient in ISO and OECD standards for toxicity

assessments. To minimize a possible detection of RNA species degraded from dying cells at this toxicity level, the culture dishes were thoroughly washed three times by PBS before harvesting to remove the dead cells and degraded molecules. For the gene expression microarray experiment, 40 mg/ml of silver-NP-hydrogel was used. The cells were seeded at a concentration of 5×10^5 cells/35-cm cell culture dish for CBMN assay, MTT assay and DNA microarray experiment. The cells were exposed to the silver-NP-hydrogel for 24 and 48 h, respectively.

CBMN assay

The CBMN assay was carried out using the protocol described as below. Briefly, the HeLa cells were seeded and maintained to 70–80% confluence at 24 h. Silver-NP-hydrogel was added to culture media at concentrations of 20, 40 and 60 mg/ml respectively, and after ultrasonic treatment (300 W, 42 kHz for 10 min) the media with silver-NP-hydrogel was applied to the cells. MMC (0.1 μg/ml) was used as a positive control, and NaCl (50 μl/ml) was used as a negative control. The cells were then further cultured for 24 h. After washing thoroughly with three times of PBS, Cytochalasin-B (final conc., 3 μg/ml) was added to the cells, and the cells were cultured for another 18 h. The cells were subsequently collected. After a hypotonic treatment in 2 ml of 0.075 M KCl at room temperature for 5 min, the cells were fixed using methyl alcohol:acetic acid (3:1). The cells were then placed onto a slide, dried at room temperature, and stained using 4% Giemsa solution (pH 6.8) for 30 min.

The slides were scored at 400× magnification blindly by two investigators separately. The micronucleation frequency (MNF, %) was determined for 1000 binucleated cells (BNCs).

Total RNA isolation and DNA microarray

The cells reached 70–85% confluence at both 24 h and 48 h cultures with the treatment of silver-NP-hydrogel at a concentration of 40 mg/ml, and almost a full conference in the control cultures with non-treatment (Figure 2). The total RNA from each sample was extracted from the HeLa cells using ISOGEN RNA isolation reagent (Nippon gene, Japan) according to the instructions provided by the manufacturer. After decontamination treatment of genomic DNA using DNase I digestion, the quality and integrity of the RNA samples were determined by appearance of the distinct 28 S and 18 S bands of ribosomal RNA on agarose gel electrophoresis. Total RNA purity was measured spectrophotometrically by the absorbance ratio 260/280 nm. Results ranged between 1.7–2.1.

A gene expression study was conducted using "Two-color microarray-based gene expression analysis" (Agilent technologies, USA, Whole Human Genome Microarray 4x44K, G4110F containing 41000 of DNA oligomer unique probes). Briefly, 1 μg of each sample of RNA was amplified using an Amino Allyl MessageAmp II aRNA Amplification Kit (Ambion, USA). Amplified RNA (aRNA) was labeled using Cy5 and Cy3 according to the instructions provided by the manufacturer. The silver-NP-hydrogel or hydrogel-alone exposure samples were labeled with Cy5, and untreated cells were labeled with Cy3 which was used as control against the treated Cy5-labeled sample. After hybridizing the samples for 16 h at 65°C, the gene chips were washed. The hybridized chips were fluorescently scanned with a microarray scanner (GenePix 4000B, USA) to collect the images. The ratios of intensity (Log_2Cy5/Cy3) were calculated and normalized with GenePixPro 6.1 software. Filtering of the results was done as follows: genes were considered as up-regulated when the Log_2Cy5/Cy3 ratio was higher than 1 (Cy5/Cy3 was higher than 2) and as down-regulated when the Log_2Cy5/Cy3 ratio was lower than −1 (Cy5/Cy3 was lower than −2). Genes were considered as unregulated when the Log_2Cy5/Cy3 ratio was between 1 and −1. The GO pathway data was further classified into functional categories. The genes, which were consistently up-regulated and down-regulated at 48 h of silver-NP-hydrogel exposure, were tabled for further analysis.

Gene ontology analysis of gene expression

To determine biological relevant gene ontology terms (GO, provided by NCBI) of differentially expressed genes in HeLa cells, the software "PANTHER", was used. It provides gene expression data analysis/Comparison of gene lists (http://www.pantherdb.org/tools/genexAnalysis.jsp). The analysis was performed using Unigene ID as the identifier for biological process categories.

Real-time PCR

The reliability of the gene expression profile was validated by real-time PCR (SYBR Green method) for five selected genes, viz., interleukin 1, alpha (IL1A); heme oxygenase (decycling) 1(HMOX1); DNA-damage-inducible transcript 3 (DDIT3); metallothionein 1 F (MT1F) and platelet-derived growth factor receptor, beta polypeptide (PDGFRB)

Table 5 Primers used in real-time PCR

Gene	GeneBank	Primer Sequence 5′→3′
Actin	NM 001101	Forward Primer: CATGTACGTTGCTATCCAGGC Reverse Primer: CTCCTTAATGTCACGCACGAT
MT1F	NM 005949	Forward Primer: CCCACTGCTTCTTCGCTTCT Reverse Primer: GAGAAAGGTTGTCCTGGCATC
IL1A	NM 000575	Forward Primer: AATGACGCCCTCAATCAAAGTA Reverse Primer: CTCCTTCAGCAGCACTGGTTG
HMOX 1	NM002133	Forward Primer: AAGAGGCCAAGACTGCGTTC Reverse Primer: GAGTGTAAGGACCCATCGGAGA
DDIT 3	NM 004083	Forward Primer: GTCCTGTCTTGATGAAAATGG Reverse Primer: GTGCTTGTGACCTCTGCTGG
PDGFRB	NM 002609	Forward Primer: GAGACTGTTGGGCGAAGGTTA Reverse Primer: GAGATGGTTGAGGAGGTGTTGAC

at 48 h exposure of silver-NP-hydrogel. Real-time PCR was performed using the ABI 7900 HT Fast RealTime PCR system (Applied Biosystem, USA). Briefly, total RNA (25 μg) from each sample was DNase I digested by the following reactions: RQ1 RNase-Free DNase 10× Reaction Buffer (5 μl), RQ1 RNase-Free DNase I (2 μl,Promega, USA), Recombinant RNasin RNase Inhibitor (1 μl, Promega, USA), Nuclease-Free Water to total volume 50 μl, with incubation for 30 min at 37°C. Following purification of DNase I digested RNA, 2 μg of RNA was reverse-transcribed into cDNA by using M-MLV reverse transcriptase (Invitrogen, USA). One μl of the cDNA sample was added to the PCR mixture which was composed of 10 μl of Power SYBR Green PCR Master Mix (Applied Biosystem, USA), 0.5 μl of forward primer (10 μM) and 0.5 μl of reverse primer (10 μM). Nuclease-free water was added to bring the volume up to 20 μl, and the mixture was subjected to PCR amplification. The primers used in this study are listed in Table 5. The threshold cycles (Ct) in each sample were measured by comparing their amplification with that of standard samples and was normalized to that of the housekeeping gene actin. An average Ct of triplicate detection for each gene, ΔCt (Detecting gene - House keeping gene); and ΔΔCt (Test sample-Control sample) was obtained; finally calculated $2^{-\Delta\Delta Ct}$ and represented as the differential expression of test genes.

Statistical analysis

The data were represented as the mean ± SD. The CBMN assay was repeated three independent times. The data was statistically analyzed using the SPSS, version 12.0.1), the *t*-test, ANOVA and Dunnett test (2-sided). Differences were considered significant if the *P*-value was less than 0.05.

Additional files

Additional file 1: Up-regulated genes in cells exposed to silver-NP-hydrogel for 24 h. Fold-change is logarithmic ratio (log2 ratio) to expression level in control.

Additional file 2: Down-regulated genes in cells exposed to silver-NP-hydrogel for 24 h. Fold-change is logarithmic ratio (log2 ratio) to expression level in control.

Additional file 3: Up-regulated genes in cells exposed to silver-NPs-hydrogel for 48h. Fold-change is logarithmic ratio (log2 ratio) to expression level in control.

Additional file 4: Down-regulated genes in cells exposed to silver-NPs-hydrogel for 48h. Fold-change is logarithmic ratio (log2 ratio) to expression level in control.

Additional file 5: Up-regulated genes in cells exposed to Hydrogel for 24 h. Fold-change is logarithmic ratio (log2 ratio) to expression level in control.

Additional file 6: Down-regulated genes in cells exposed to Hydrogel for 24 h. Fold-change is logarithmic ratio (log2 ratio) to expression level in control.

Additional file 7: Up-regulated genes in cells exposed to Hydrogel for 48h. Fold-change is logarithmic ratio (log2 ratio) to expression level in control.

Additional file 8: Down-regulated genes in cells exposed to Hydrogel for 48 h. Fold-change is logarithmic ratio (log2 ratio) to expression level in control.

Additional file 9: Common up-regulated genes in cells exposed to silver-NP-hydrogel for 24 h and 48 h. Fold-change is logarithmic ratio (log2 ratio) to expression level in control.

Additional file 10: Common down-regulated genes in cells exposed to silver-NP-hydrogel for 24h and 48 h. Fold-change is logarithmic ratio (log2 ratio) to expression level in control.

Additional file 11: Common up-regulated genes in cells exposed to hydrogel for 24 h and 48 h. Fold-change is logarithmic ratio (log2 ratio) to expression level in control.

Additional file 12: Common down-regulated genes in cells exposed to hydrogel for 24 h and 48 h. Fold-change is logarithmic ratio (log2 ratio) to expression level in control.

Additional file 13: Common up-regulated genes in cells exposed to hydrogel and silver-NP-hydrogel for 48h. Fold-change is logarithmic ratio (log2 ratio) to expression level in control.

Additional file 14: Common down-regulated genes in cells exposed to hydrogel and silver-NP-hydrogel for 48h. Fold-change is logarithmic ratio (log2 ratio) to expression level in control.

Additional file 15: Down-regulated genes related to mitosis pathway at silver-NP-hydrogel treatment for 48h.

Additional file 16: Figure S1. The size and size distribution of the silver nanoparticles determined by transmission electron microscopy (TEM). A: X 10000, bar = 200 nm; B: X 20000, bar = 100 nm.

Abbreviations

silver-NP: Silver nanoparticle; silver-NP-hydrogel: Silver nanoparticle based hydrogel; CBMN: Cytokinesis-block micronucleus; ROS: Reactive oxygen species; Cyto-B: Cytochalasin B; DMSO: Dimethyl sulfoxide; MMC: Mitomycin C; MTT: Methyl tetrazolium; GO: Gene ontology; MNF: Micronucleation frequency; BNCs: Binucleated cells; TEA: Triethanolamine; CDC14A: Cell division cycle 14 homolog A; JAK-STAT: Janus kinase/signal transducers and activators of transcription; IFI: Interferon-induced proteins; IFIT: Interferon-induced protein in the tetratricopeptide; IL: Interleukin; IL1A: Interleukin 1 alpha; HMOX1: Heme oxygenase (decycling); DDIT3: DNA-damage-inducible transcript 3; MT1F: Metallothionein 1 F; PDGFRB: Platelet-derived growth factor receptor beta polypeptide.

Competing interests

The authors declare that they have no competing interests.

Acknowledgements

This study was financially supported by the Human Resources and Social Security Office of China (HRSSO Letter [2009], No. 416), the Beijing Natural Science Foundation of China (No. 3112024) and the Open Research Fund of State Key Laboratory of Bioelectronics, Southeast University, China; National Key Technology Research and Development Program of the Ministry of Science and Technology of China (2012BAI22B01, 2012BAK26B00).

Author details

[1]Institute for Medical Devices Control, National Institutes for Food and Drug Control (NIFDC), No. 2 Temple of Heaven, Beijing 100050, China. [2]Baotou Medical College, Inner Mongolia University of Science & Technology, Baotou 014010, China. [3]Interdisciplinary Laboratory for Nanoscale Science and Technology, National Institute for Materials Science, 1-2-1 Sengen, Tsukuba, Ibaraki 305-0047, Japan. [4]Goldman School of Dental Medicine, Boston University, 801 Albany Street, Suite 200, Boston, MA 02118-2392, USA.

Authors' contributions

Liming Xu participated in the design of study, sequence alignment, performed the statistical analysis and drafted the manuscript. Xuefei Li carried out the genotoxic assay, participated in the sequence alignment and drafted the manuscript. Taro Takemura and Nobutaka Hanagata carried out

the DNA microarray experiment and data analysis. Gang Wu and Laisheng Lee Chou participated in the design of study, data analysis and coordination, and drafting manuscript. All authors read and approved the final manuscript.

Received: 7 December 2011 Accepted: 1 May 2012
Published: 1 May 2012

References

1. Lee JH, Chae JD, Kim DG, Hong SH, Lee WM, Ki M: **Comparison of the efficacies of silver-containing dressing materials for treating a full-thickness rodent wound infected by methicillin-resistant Staphylococcus aureus.** *Korean J Lab Med* 2010, **30**:20–27.
2. Elliott C: **The effects of silver dressings on chronic and burns wound healing.** *Br J Nurs* 2010, **19**:S32–S36.
3. Gabriel MM, Mayo MS, May LL, Simmons RB, Ahearn DG: **In vitro evaluation of the efficacy of a silver-coated catheter.** *Curr Microbiol* 1996, **33**:1–5.
4. Ahearn DG, Grace DT, Jennings MJ, Borazjani RN, Boles KJ, Rose LJ, Simmons RB, Ahanotu EN: **Effects of hydrogel/silver coatings on in vitro adhesion to catheters of bacteria associated with urinary tract infections.** *Curr Microbiol* 2000, **41**:120–125.
5. Wu J, Hou S, Ren D, Mather PT: **Antimicrobial properties of nanostructured hydrogel webs containing silver.** *Biomacromolecules* 2009, **10**:2686–2693.
6. Gils PS, Ray D, Sahoo PK: **Designing of silver nanoparticles in gum arabic based semi-IPN hydrogel.** *Int J Biol Macromol* 2010, **46**:237–244.
7. Thomas V, Yallapu MM, Sreedhar B, Bajpai SK: **A versatile strategy to fabricate hydrogel-silver nanocomposites and investigation of their antimicrobial activity.** *J Colloid Interface Sci* 2007, **315**:389–395.
8. Ji JU, Jung JH, Kim SS, Yoon JU, Park JD, Choi BS, Chung YH, Kwon IU, Jeong J, Han BS, Shin JH, Sung JH, Song KS, Yu IJ: **Twenty-eight-day inhalation toxicity study of silver nanoparticles in Sprague–Dawley rats.** *Inhal Toxicol* 2007, **19**:857–871.
9. Sung JH, Ji JH, Yoon JU, Kim DS, Kim DS, Song MY, Jeong J, Han BS, Han JH, Chung YH, Kim J, Kim TS, Chang HK, Lee EJ, Lee JH, Yu IJ: **Lung function changes in Sprague–Dawley rats after prolonged inhalation exposure to silver nanoparticles.** *Inhal Toxicol* 2008, **20**:567–574.
10. Sung JH, Ji JH, Park JD, Yoon JU, Kim DS, Jeon KS, Song MY, Jeong J, Han BS, Han JH, Chung YH, Chang HK, Lee JH, Cho MH, Kelman BJ, Yu IJ: **Subchronic inhalation toxicity of silver nanoparticles.** *Toxicol Sci* 2009, **108**:452–461.
11. Kim YS, Kim JS, Cho HS, Rha DS, Kim JM, Park JD, Choi BS, Lim R, Chang HK, Chund YH, JKwon IH, Jeong J, Han BS, Yu IJ: **Twenty-eight-day oral toxicity, genotoxicity, and gender-related tissue distribution of silver nanoparticles in Sprague–Dawley rats.** *Inhal Toxicol* 2008, **20**:575–583.
12. Kim YS, Song MY, Park JD, Song KS, Ryu HR, Chung YH, Chang HK, Lee JH, Oh KH, Kelman BJ, Hwang IK, Yu IJ: **Subchronic Oral toxicity of silver nanoparticles.** *Part Fibre Toxicol* 2010, **7**:20.
13. Tang J, Xiong L, Wang S, Wang J, Liu L, Li J, Yuan F, Xi T: **Distribution, translocation and accumulation of silver nanoparticles in rats.** *J Nanosci Nanotechnol* 2009, **9**:4924–4932.
14. Tang J, Xiong L, Zhou G, Wang S, Wang J, Liu L, Jiage Li, Yuan F, Lu S, Wan Z, Chou L, Xi T: **Silver nanoparticles crossing through and distribution in the blood–brain barrier in vitro.** *J Nanosci Nanotechnol* 2010, **10**: 6313–6317.
15. Braydich-Stolle L, Hussain S, Schlager JJ, Hofmann MC: **In vitro cytotoxicity of nanoparticles in mammalian germline stem cells.** *Toxicol Sci* 2005, **88**:412–419.
16. Crewlich C, Kittler S, Epple M, Muhr G, Koller M: **Studies on the biocompatibility and the interaction of silver nanoparticles with human mesenchymal stem cells (hMSCs).** *Langenbecks Arch Surg* 2009, **394**: 495–502.
17. Hackenberg S, Scherzed A, Kessler M, Hummel S, Technau A, Froelich K, Ginzkey C, Koehler C, Hagen R, Kleinsasser N: **Silver nanoparticles: evaluation of DNA damage, toxicity and functional impairment in human mesenchymal stem cells.** *Toxicol Lett* 2010, **201**:27–33.
18. Greulich C, Diendorf J, Simon T, Eggeler G, Epple M, Köller M: **Uptake and intracellular distribution of silver nanoparticles in human mesenchymal stem cells.** *Acta Biomater* 2011, **7**:347–354.
19. Hussain SM, Hess KL, Gearhart JM, Geiss KT, Schlager JJ: **In vitro toxicity of nanoparticles in BRL 3A rat liver cells.** *Toxicol In Vitro* 2005, **19**:975–983.
20. Hsin YH, Chen CF, Huang S, Shih TS, Lai PS, Chueh PJ: **The apoptotic effect of nanosilver is mediated by a ROS- and JNK-dependent mechanism involving the mitochondrial pathway in NIH3T3 cells.** *Toxicol Lett* 2008, **179**:130–139.
21. Kawata K, Osawa M, Okabe S: **In vitro Toxicity of silver nanoparticles at nanocytotoxic doses to HepG2 human hepatoma cells.** *Environ Sci Technol* 2009, **43**:6046–6051.
22. AshaRani PV, Hande PM, Valiyaveettil S: **Anti-proliferative activity of silver nanoparticles.** *BMC Cell Biology* 2009, **10**:65–79.
23. AshaRani PV, Low Kah MG, Hande MP, Valiyaveettil S: **Cytotoxicity and genotoxicity of silver nanoparticles in human cells.** *ACS nano* 2009, **3**: 279–290.
24. Kim HR, Kim MJ, Lee SY, Oh SM, Chung KH: **Genotoxic effects of silver nanoparticles stimulated by oxidative stress in human normal bronchial epithelial (BEAS-2B) cells.** *Mutat Res* 2011, **726**:129–135.
25. Xu L, Takemura T, Xu M, Hanagata N: **Toxicity of silver nanoparticles as assessed by global gene expression analysis.** *Materials Express* 2011, **1**: 74–79.
26. Kumari M, Mukherjee A, Chandrasekaran N: **Genotoxicity of silver nanoparticles in Allium cepa.** *Sci Total Environ* 2009, **407**:5243–5246.
27. Boonstra J, Post JA: **Molecular events associated with reactive oxygen species and cell cycle progression in mammalian cells.** *Gene* 2004, **337**: 1–13.
28. Xia T, Kovochich M, Brant J, Hotze M, Sempf J, Oberley T, Sioutas C, Yeh JI, Wiesner MR, Nel AE: **Comparison of the abilities of ambient and manufactured nanoparticles to induce cellular toxicity according to an oxidative stress paradigm.** *Nano Lett* 2006, **6**:1794–1807.
29. Carlson C, Hussain SM, Schrand AM, Braydich-Stolle LK, Hess KL, Jones RL, Schlager JJ: **Unique cellular interaction of silver nanoparticles: size-dependent generation of reactive oxygen species.** *J Phys Chem* 2008, **112**:13608–13619.
30. Fenech M: **The advantages and disadvantages of the cytokinesis-block micronucleus method.** *Mutat Res* 1997, **392**:11–18.
31. Chou L: **Molecular biocompatibility.** *J Dent Res* 1995, **74**:190–193.
32. Lu X, Bao X, Huang Y, Qu Y, Lu H, Lu Z: **Mechanisms of cytotoxicity of nickel ions based on gene expression profiles.** *Biomaterials* 2009, **30**: 141–148.
33. Lu X, Lu H, Zhao L, Yang Y, Lu Z: **Genome-wide pathways analysis of nickel ion-induced differential genes expression in fibroblasts.** *Biomaterials* 2010, **31**:1965–1973.
34. Kim JS, Sung JH, Ji JH, Song KS, Lee JH, Kang CS, Yu IJ: **In vivo genotoxicity of silver nanoparticles after 90-day silver nanoparticle inhalation exposure.** *Saf Health Work* 2011, **2**:34–38.
35. Xu L, Chen L, Dong Z, Wang J, Wang Z, Shao A: **In vivo toxicity in reproductive organs of rabbit and in vitro cytotoxicity of silver nanoparticle based-hydrogel.** *Chi J Pharm Anal* 2012, **2**:194–201.
36. Becker H, Herzberg F, Schulte A, Kolossa-Gehring M: **The carcinogenic potential of nanomaterials, their release from products and options for regulating them.** *Int J Hyg Environ Health* 2011, **214**:231–238.
37. Sanchez VC, Pietruska JR, Miselis NR, Hurt RH, Kane AB: **Biopersistence and potential adverse health impacts of fibrous nanomaterials: what have we learned from asbestos?** *Wiley Interdiscip Rev Nanomed Nanobiotechnol* 2009, **1**:511–529.
38. Tsui MT, Wang WX: **Biokinetics and tolerance development of toxic metals in Daphnia magna.** *Environ Txicol Chem* 2007, **26**:1023–1032.
39. Min KS: **Physiological significance of metallothionein in oxidative stress.** *Yakugaku Zasshi* 2007, **127**:695–702.
40. Woo S, Yum S, Jung JH, Shim WJ, Lee CH, Lee TK: **Heavy metal-induced differential gene expression of metallothionein in Javanese medaka, Oryzial javanicus.** *Mar Biotechnol (NY)* 2006, **8**:654–662.
41. Clark JE, Foresti R, Green CJ, Motterlini R: **Dynamics of haem oxygenase-1 expression and bilirubin production in cellular protection against oxidative stress.** *Biochem J* 2000, **384**:615–619.
42. Elbirt KK, Bonkovsky HL: **Heme oxygenase: recent advances in understanding its regulation and role.** *Proc Assoc Am Physicians* 1999, **111**:438–447.
43. Rahman MF, Wang J, Patterson TA, Saini UT, Robinson BL, Newport GD, Murdock RC, Schlager JJ, Hussain SM, Ali SF: **Expression of genes related to oxidative stress in the mouse brain after exposure to silver-25 nanoparticles.** *Toxicol Lett* 2009, **187**:15–21.
44. Wong AK, Chen Y, Lian L, Ha PC, Petersen K, Laity K, Carillo A, Emerson M, Heichman K, Gupte J, Tavtigian SV, Teng DH: **Genomic structure, chromosomal location, and mutation analysis of the human CDC14A gene.** *Genomics* 1999, **59**:248–251.

45. Aaronson DS, Horvath CM: **Road Map for Those Who Don't Know JAK-STAT.** *Science* 2002, **296**:1653–1655.
46. O'Shea JJ, Gadina M, Schreiber RD: **Cytokine Signaling: new Surprises in the Jak/Stat Pathway.** *Cell* 2002, **109**:S121–S131.
47. Imada K, Leonard WJ: **The Jak-STAT pathway.** *Mol Immunol* 2000, **37**:1–11.
48. Hebenstreit D, Horejs-Hoeck J, Duschl A: **JAK/STAT-dependent gene regulation by cytokines.** *Drug News Perspect* 2005, **18**:243–249.
49. Espert L, Dusanter-Fourt I, Chelbi-Alix MK: **Negative regulation of the JAK/STAT: pathway implication in tumorigenesis.** *Bull Cancer* 2005, **92**:845–857.
50. Rakesh K, Agrawal DK: **Controlling cytokine signaling by constitutive inhibitors.** *Biochem Pharmacol* 2005, **70**:649–657.

doi:10.1186/1477-3155-10-16
Cite this article as: Xu *et al.*: Genotoxicity and molecular response of silver nanoparticle (NP)-based hydrogel. *Journal of Nanobiotechnology* 2012 **10**:16.